clone producing non-neutralizing antibodies from a well-characterized HCV-carrier (patient H). Isolation and characterization of these human monoclonal antibodies are detailed in this report.

Materials and Methods

Peripheral Blood Mononuclear Cells (PBMC) and Cell Lines

Following written informed consent, the blood sample was obtained in 2000 from patient H who developed chronic HCV infection after transfusion in 1977 [12]. The work was conducted with approval from the Institutional Review Board of the Clinical Center, National Institutes of Health, Bethesda, USA. (IRB # 91-CC-0117). PBMC were isolated by Ficoll-Isopaque (Pharmacia, Uppsala, Sweden), washed three times in phosphate-buffered saline (PBS), re-suspended in Cell Culture Freezing Medium (Life Technologies Japan, Tokyo, Japan), and stored at −80°C until use. Huh 7 cells, a cell line derived from a hepatocellular carcinoma, and highly permissive Huh7.5 cells [13] (provided by C. Rice, Rockefeller University, USA) were cultured in Dulbecco's modified Eagle's medium (DMEM) (Wako, Tokyo, Japan) supplemented with 10% fetal bovine serum (FBS) (Nichirei, Tokyo, Japan). Cells were grown at 37°C in a CO_2 incubator.

Immunofluorescence (IF)

After fixation in ice-cold 100% acetone for 5 min, cells were incubated with primary antibody for 30 min at room temperature, washed 3 times in PBS, and incubated with a 1:200 dilution of the AlexaFluor 488 (Invitrogen, Carlsbad, CA, USA) secondary antibody for 30 min at room temperature. The samples were examined under a TE200 fluorescence microscope (Nikon, Tokyo, Japan).

Equilibrium Centrifugation in Sucrose Density Gradient (SDG)

A crude supernatant containing HCV was centrifuged at 2,380×g for 15 min at 4°C, filtered through the 0.45 µm membrane, concentrated approximately 100-fold using Amicon Ultra-15 centrifugal filter unit with Ultracel-100 (100 kD cut-off) membrane (Millipore, Billerica, MA, USA). The concentrated sample (1.5 ml) was overlaid on 6 ml of a discontinuous gradient with 10, 20, 30, 40, 50, and 60% (w/v) sucrose steps and centrifuged at 289,000×g for 20 h at 4°C in a CS 100GXL centrifuge (Hitachi, Tokyo, Japan). Buoyant density of fractions was determined by refractometry and expressed in g/ml.

Immuno-gold Electron Microscopy (EM)

For preparing a concentrated virus sample, fraction 3 obtained from the SDG centrifugation described above was diluted in 6.5 ml PBS and spun down at 215,000×g for 4 h at 4°C in a S58A-0015 rotor (Hitachi, Tokyo, Japan). The resulting pellet was suspended in 50 µl of PBS, mixed with an equal volume of antibody #55, #37, or a control antibody (500 µg/ml), and incubated overnight at 4°C. The mixture was then treated with 10 µl of goat anti-human IgG conjugated with colloidal gold-particles (Jackson Labs, Grove, PA, USA) overnight at 4°C. The sample was placed on a high resolution carbon grid, STEM100Cu (Oken, Tokyo, Japan), negatively stained with 2% uranyl acetate solution, and examined under a JEM-100C transmission electron microscope (JEOL, Tokyo, Japan) at 100 kV.

Reverse-transcription (RT), PCR, and Quantitative PCR (qPCR)

Extraction of RNA, RT, and PCR were carried out as described previously [14]. The amount of HCV cDNA was measured by qPCR using SYBR Premix Ex Taq (Takara, Tokyo, Japan) with an ABI Prism model Fast 7700 instrument (Applied Biosystems, Tokyo, Japan). To determine copy numbers, standard curves were prepared with serial 10-fold dilutions of a known amount of a plasmid bearing the amplified HCV sequence. We used primers that amplified the 5′ non-coding region of the viral genome. The sequences of the primers used were 5′-TTC ACG CAG AAA GCG TCT AG-3′ as a sense primer and 5′-CCC TAT CAG GCA GTA CCA CA-3′ as an anti-sense primer [15]. For detection of RNA encoding the V_H regions of antibodies, we used primer pair CG1z (5′-GCA TGT ACT AGT TTT GTC ACA AGA TTT GGG-3′) and VH6a (5′-CAG GTA CAG CTC GAG CAG TCA GG-3′) for #37, and primer pair CG1z and VH3a (5′-GAG GTG CAG CTC GAG GAG TCT GGG-3′) for #55. The RT-PCR products were cloned into pCR4TOPO (Invitrogen, Carlsbad, CA, USA) and the molecular clones were sequenced with an ABI PRISM^{TM}310 Genetic Analyzer (Applied Biosystems, Tokyo, Japan).

Expression of HCV E2 Proteins

Forns et al., [16] reported that the HCV E2 protein, when expressed on the cell surface, acquired its native conformation more efficiently when truncated at amino acid (aa) 661 of the viral genome. Therefore, we prepared expression vectors encoding truncated forms of E2 (aa 384 to 661) derived from HCV isolates of patient H, obtained in 1977 (strain H77, AF011751) and in 2000 (strain H00) for the screening of antibody-positive clones. For epitope mapping, we prepared vectors encoding various sizes of E2 proteins derived from strain H77. The inserts were amplified by RT-PCR, cloned into pDisplay (Invitrogen, Carlsbad, CA, USA) in frame between a signal sequence and a trans-membrane domain. All clones were sequenced to ensure that the DNA encoded the authentic HCV sequence. Huh 7 cells were grown in Lab-Tek 8-chamber slides (Nagle Nunc, Naperville, IL, USA) until 80% confluent and transfected with the constructs using SuperFect (Qiagen, Valencia, CA, USA) according to the manufacturer's instructions. After 48 h, cells were washed, fixed with cold acetone for 5 min, and stored at −80°C until use. Expression of the E2 proteins was verified by IF with rabbit hyperimmune sera raised against various domains of HCV E2.

HCV Plasmids and Generation of Infectious HCV

Plasmid pJFH1 that contains full-length cDNA of HCV strain JFH1 was provided by T. Wakita (National Institute of Infectious Diseases, Tokyo, Japan) [5]. Plasmids pFK-JFH/Con1/C-842-dg, pFK-JFH/J6/C846-dg, and pFK-JFH1/H77/C842-dg to generate chimeric infectious HCV Con1/C3, J6/C3, and H77/C3, respectively, were given by R. Bartenschlager (University of Heidelberg, Heidelberg, Germany) [17]. Plasmids pH77C/JFH1, pJ4/JFH1, pJ6/JFH1, pJ8/JFH1, pS52/JFH1, pED43/JFH1, pSA13/JFH1, pHK6a/JFH1, and pQC69/JFH1 to generate chimeric infectious HCV were provided by J. Bukh (Copenhagen University Hospital, Hvidovre, Denmark) [18–22]. These chimeras are JFH1-based recombinants expressing core-NS2 of genotype 1 to 7 isolates. For the synthesis of HCV RNA, the plasmids were transcribed using a Megascript T7 kit (Ambion, Austin, TX, USA). To generate infectious HCV, the *in vitro* transcribed viral genomic RNA was transfected into

Huh7.5 cells by electroporation using a Gene Pulser system (Bio-Rad, Hercules, CA, USA) or by using Lipofectamine 2000 reagent (Invitrogen, Carlsbad, CA, USA) as described by the manufacturer. The culture supernatants collected at 2–7 days after transfection were centrifuged, passed through a 0.45 μm filter, and inoculated into naïve Huh7.5 cells. After additional passages on naïve cells, the cell-free supernatants containing HCV were concentrated approximately 10-fold using Amicon Ultra-15 (Millipore, Billerica, MA, USA) and measured for their infectivity titers. Aliquots were stored at −80°C until use.

Infectivity Titration

Virus titers were determined by focus-forming units (FFU) assay. Huh7.5 cells were seeded at 2×10^5 cells per well in 24-well plates and cultured overnight. Test samples were diluted serially 10-fold and each dilution was inoculated into the cells. After incubation for 6 h at 37°C, the cells were supplemented with fresh complete DMEM and cultured for 24 h. The cells were then immuno-stained and HCV-positive foci were manually counted under a fluorescence microscope. Each test was performed in duplicate or triplicate. The virus titer was expressed in FFU per ml sample, as determined by the mean number of IF-positive foci detected in a whole well.

Virus Neutralization Assays

Neutralization of HCV infection was assessed by the FFU reduction assay. Two independent assays were performed in the different laboratories. The first method was as follows: A 0.5 ml of serial 5-fold dilutions of #37, #55, or an irrelevant control antibody (human-IgG) (Sigma-Aldrich, St. Louis, MO, USA) was pre-incubated at 4°C overnight with an equal volume of the virus solution containing approximately 300 FFU/ml of HCV. The mixtures were inoculated into Huh7.5 cells (5×10^5/well) cultured on a 15mm-coverglass in 12-well plates. After incubation for 48 h, cells on the glass were fixed with cold 100% acetone and subjected to indirect IF for the detection of infected foci using a serum from patient H followed by the AlexaFluor 488 secondary antibody. IF-positive foci on the whole coverglass were manually counted under a fluorescence microscope. Each test was performed in duplicate. The second method was as follows: A 0.1 ml of the dilutions containing 0.2, 1, 3, 10, 30, 100, 300, or 1000 μg/ml of #55 or a control antibody was pre-incubated at 37°C for 1 h with an equal volume of the virus solution containing 10^2 or 10^3 FFU/0.1 ml of HCV. The mixtures were inoculated onto Huh7.5 cells (10^5 cells/well in 24-well plates). After 3 h of adsorption, the inocula were removed and fresh complete DMEM were added to the wells. At 24 h post-infection, cells were fixed with 4% paraformaldehyde (Wako, Tokyo, Japan) followed by permeabilization with 0.1% Triton-100 (Wako, Tokyo, Japan). The cells were then immuno-stained for the HCV proteins, counterstained with Hoechst 33342 (Invitrogen, Carlsbad, CA, USA), and examined under a BZ-9000 fluorescence microscope (Keyence, Osaka, Japan). The number of HCV infected cells in each well was manually counted. The percent neutralization was calculated as the percent reduction of FFU compared with virus incubated with the control antibody. The NT_{50} value, lowest concentration (μg/ml) of antibody required for 50% reduction of FFU, was determined by curvilinear regression analysis.

Results

Establishment of Human Lymphoblastoid Cell Lines Producing Monoclonal Antibodies to the Envelope E2 Protein of HCV

PBMC obtained from patient H were infected with Epstein-Barr virus, strain B95-8, as we described previously [23], and cultured at 37°C in a 75 ml-flask in medium RPMI1640 (Life Technologies Japan, Tokyo, Japan) containing 10% FBS. Ten days later, the cells were distributed in 96-well plates in an amount of 10^4 cells/0.2 ml/well. After 4 days of cultivation, supernatant from each well was screened for presence of antibodies by IF using Huh 7 cells expressing the E2 protein (aa 384 to 661) derived from HCV strain H77. Cells in the well that gave a positive signal were re-distributed into 96-well plates and the wells were screened again. This procedure was repeated 5 times until all of the tested wells became positive on two successive assays. When cellular RNA was extracted and the V_H region of antibody was amplified by RT-PCR, identical sequence was obtained from three randomly selected wells, suggesting that the cells were clones. Antibody from this clone was designated as #37.

With a similar procedure we obtained antibody #55. For the screening of #55, Huh7 cells expressing the E2 protein derived from HCV strain H00 was employed as a target. **Figure 1** shows deduced amino acid sequences of the V_H regions for #37 and #55. The antibodies were isotyped by IF with Huh7 cells expressing the E2 protein (aa 384–661) of HCV strain H77, using specific secondary antibodies to human IgM, IgG1, IgG2, IgG3, and IgG4 subclasses, and to lambda and kappa light chains (Binding Site Inc., San Diego, CA, USA). As shown in **Figure 2**, #37 was IgG1/kappa and #55 was IgG1/lambda. The IgG was purified from the supernatants using a HiTrap protein G HP column (GE Healthcare, Uppsala, Sweden) and used for further characterization.

Epitope Mapping

Both #37 and #55 failed to react with the E2 protein in the western blot assay. Therefore, these antibodies were considered to recognize conformational epitopes. In order to map epitope sequences, we prepared expression vectors encoding various regions of the E2 protein derived from HCV strain H77. They include the regions aa 384 to 661, aa 411 to 661, aa 429 to 652, aa 429 to 607, aa 508 to 652, aa 429 to 552, aa 508 to 607, aa 552 to 652, aa 508 to 552, and aa 552 to 607. Huh7 cells expressing these regions were tested by IF for reactivity with #37 and #55. As shown in **Figure 3**, #37 was reactive with the expressed form of the E2 protein containing aa 429 to 652, but not with smaller sizes than this region. In contrast, #55 was reactive with the truncated form down to the region aa 508 to 607. These results indicate that the target epitopes of #37 and #55 are located in the regions of aa 429 to 652 and aa 508 to 607, respectively.

Cross-reactivity with Different HCV Genotypes and Binding Ability

Recent development of infectious chimeric HCV [17–22] has made it possible to investigate cross-genotype reactivity of the antibodies utilizing virus-infected cells as a target. We examined the cross-reactivity of #37 and #55 by IF using Huh7.5 cells infected HCV with different genotype E2 proteins. Genotypes tested were 1a, 1b, 2a, 2b, 3a, 4a, 5a, 6a, and 7a. Both #37 and #55 were reactive by IF with all genotypes tested.

Binding ability of #37 and #55 was assessed by measuring the minimum concentration of the antibodies required for an IF-

MAb	FR1	CDR1	FR2
#37	QVQLEQSGGGLVKPGESLRLSCAASGFILS	HYHMS	WFRQAPGKGLEWIA
#55	E----E------Q--G------E----MF-	AGW-H	-V--------V-VS

MAb	CDR2	FR3
#37	DINYSGRTTYEADSVRG	RFTVSRDNAKWSLYLQMNSLRVEDTAMYYCAR
#55	R---D-SS-TYV---K-	----------NT-F----------V----S

MAb	CDR3	FR4
#37	VGVVASINLMVGRRRSDNWFDL	WGQGTLVTVSS
#55	G-YYSYGPFGD.....	---------P-

Figure 1. Amino acid sequences of the V_H regions of #37 and #55. Residues identical to #37 sequences are indicated by a dash. Dots indicate gaps compared with the sequence of #37. MAb, monoclonal antibody; FR, framework regions; CDR, complementarity-determining regions.
doi:10.1371/journal.pone.0055874.g001

positive reaction using HCV-infected Huh7.5 cells as targets. The HCV inocula tested were strain JFH1 (genotype 2a) and ten chimeric HCV, including H77C/JFH1 (genotype 1a), J4/JFH1 (genotype 1b), Con1/C3 (genotype 1b), J6/JFH1 (genotype 2a), J8/JFH1 (genotype 2b), S52/JFH1 (genotype 3a), ED43/JFH1 (genotype 4a), SA13/JFH1 (genotype 5a), HK6a/JFH1 (genotype 6a) and QC69/JFH1 (genotype 7a). Antibody solutions containing 5 μg/ml of IgG were two-fold serially-diluted and each dilution was tested by IF for a positive reaction. The results are shown in **Table 1**. The minimum concentration of #55 required was 10–78 ng/ml, while that of #37 was 156–1250 ng/ml except for H77C/JFH1 and S52/JFH1, which required 20 ng/ml. The higher ability of #37 in binding to H77C/JFH1 was possibly because this chimeric virus was a JFH1-based recombinant with homologous envelope E2 of strain H77 from the PBMC-donor. The higher reactivity with S52/JFH1 remains unexplained. Overall, more of #37 was needed for a positive reaction compared to #55, indicating that #55 has a higher binding ability than #37.

Distribution of Reacting Antigens in the HCV-infected Cells

Distribution of the antigens reacting with #55 and #37 in the HCV-infected cells was observed by IF-staining. We

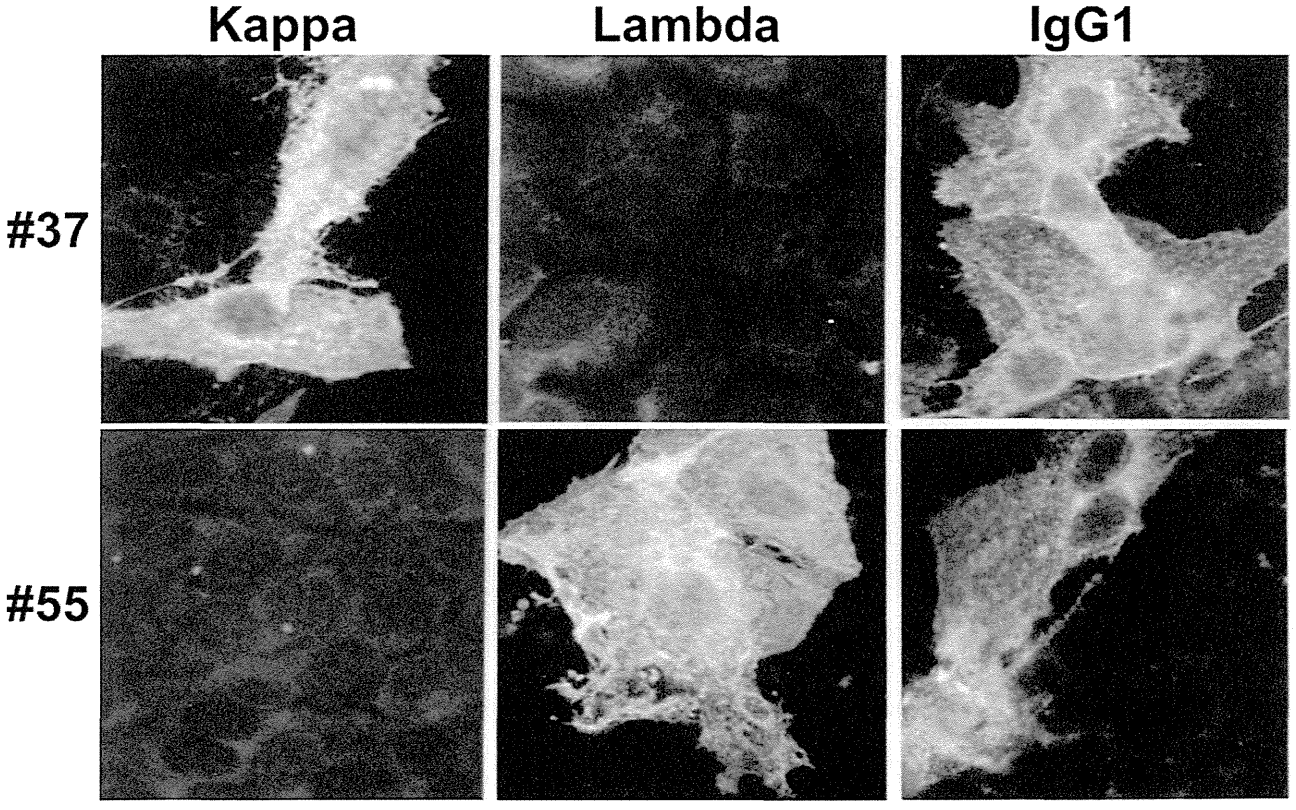

Figure 2. Isotyping revealed that #37 and #55 were IgG1/kappa and IgG1/lambda, respectively. Huh7 cells expressing the HCV E2 (aa 384–661) derived from strain H77 were incubated with #37 or #55, washed, and stained with fluoresceinated anti-human IgG1, anti-human lambda, or anti-human kappa.
doi:10.1371/journal.pone.0055874.g002

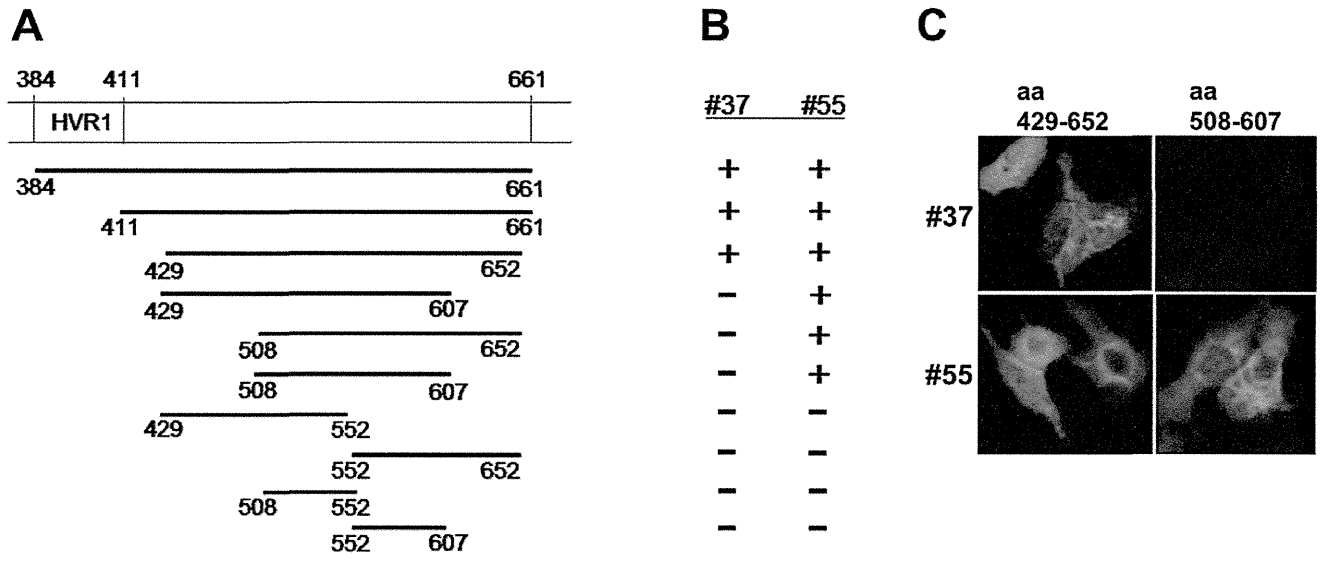

Figure 3. Epitope mapping revealed that #37 and #55 recognized the regions aa 429 to 652 and aa 508 to 607 of the E2 protein, respectively. (**A**). A panel of Huh7 cells expressing various truncations of the E2 protein derived from HCV strain H77 was generated. At the top of the graphic, aa 384 to 661 of the E2 protein is depicted with aa numbers. HVR1, hyper variable region 1. (**B**). Results of the assays for reactivity by IF. +, positive recognition; -, negative recognition. (**C**). IF-reactions of #37 and #55 against the cells expressing aa 429–652 and aa 508–607.
doi:10.1371/journal.pone.0055874.g003

examined Huh7.5 cells infected with 12 different inocula of HCV, including strain JFH1 and eleven chimeric HCV with structural proteins derived from various genotypes. **Figure 4** shows IF positive-staining by #37 and #55 observed in the cells infected with strain JFH1. The antibodies produced a different pattern of staining; while #37 gave coarse granular staining mostly located in the periphery of the nucleus, #55 gave diffuse staining throughout the cytoplasm. Similar patterns of IF-staining were observed for other chimeric HCV tested, including H77C/JFH1, J4/JFH1, J6/JFH1, J8/JFH1, S52/JFH1, ED43/JFH1, SA13/JFH1, HK6a/JFH1, QC69/JFH1, H77/C3, and Con1/C3. An irrelevant control antibody (human IgG) did not give such positive staining in the infected cells. #37, #55, and the control antibody were not reactive with non-infected Huh7.5 cells.

Ability to Recognize HCV Particles

It was recently reported that cell culture-grown HCV particles were pleomorphic, 40–75 nm in diameter, and spherical [24]. To determine whether #37 and #55 are able to recognize intact viral particles, we performed indirect immuno-gold EM using anti-human IgG labeled with colloidal gold particles as a second antibody. As target HCV for this experiment, we employed H77/C3 with homologous envelope E2 of strain H77 from the PBMC-donor. Concentration and purification of viral particles from culture supernatants was carried out by equilibrium SDG centrifugation. **Figure 5A** shows the distribution of HCV RNA measured by RT-qPCR after the centrifugation. Two peaks of viral RNA were obtained at 1.076 g/ml and 1.171 g/ml in fractions 3 and 6, respectively. Copy numbers of HCV RNA were 4.3×10^{5}/0.1 ml for fraction 3 and 7.4×10^{5}/0.1 ml for fraction 6.

Table 1. Binding activity measured by immunofluorescence.

Virus (genotype)	Minimum concentration (ng/ml) required for positive reaction	
	#37	#55
H77C/JFH1 (1a)	20	10
J4/JFH1 (1b)	156	78
J6/JFH1 (2a)	1250	20
J8/JFH1 (2b)	1250	78
S52/JFH1 (3a)	20	10
ED43/JFH1 (4a)	625	20
SA13/JFH1 (5a)	156	78
HK6a/JFH1 (6a)	156	78
QC69/JFH1 (7a)	1250	78
Con1/C3 (1b)	625	78
JFH1 (2a)	313	78

doi:10.1371/journal.pone.0055874.t001

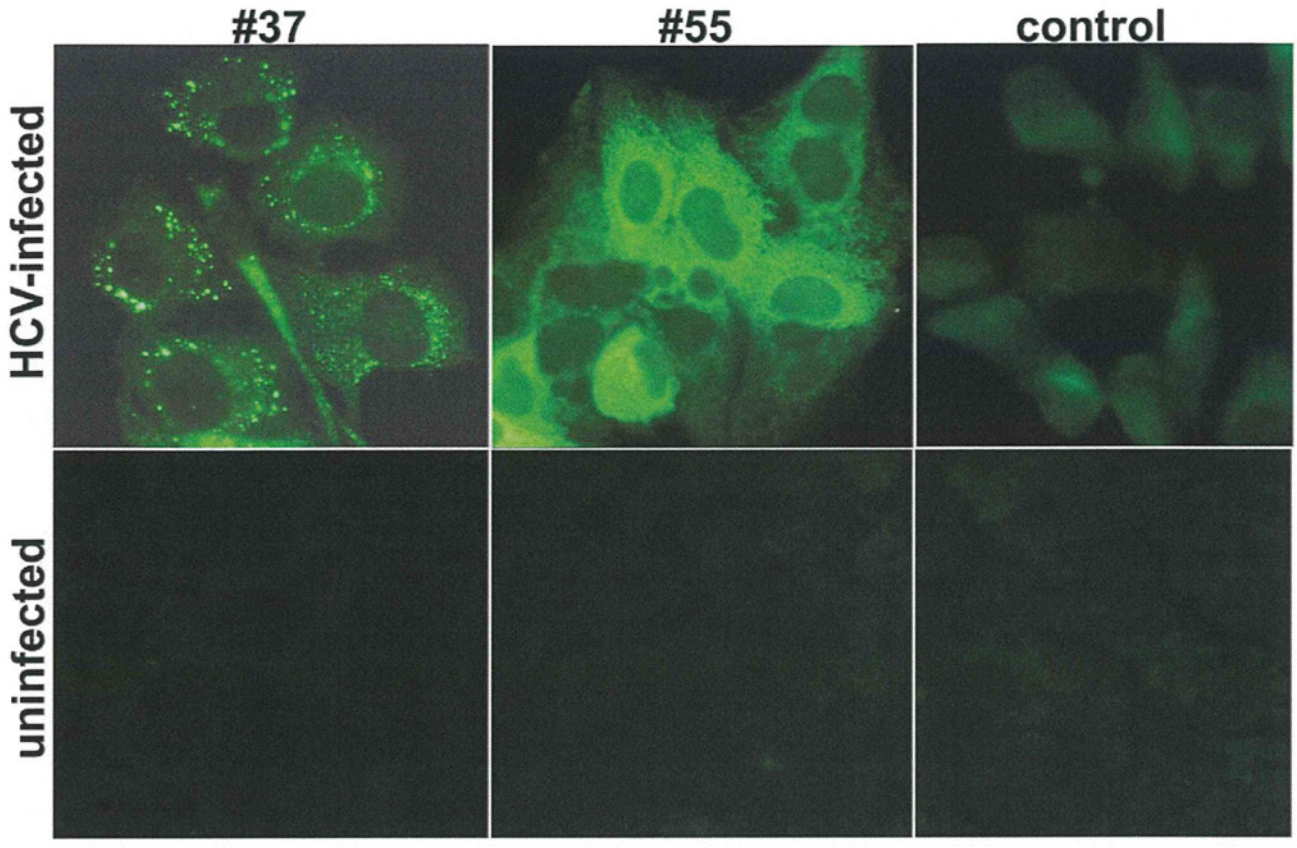

Figure 4. Different pattern of IF-staining by #37 and #55 in the HCV-infected Huh7.5 cells. #37 gave granular IF-reactions scattered in the cytoplasm. #55 gave diffuse staining throughout the cytoplasm. The control antibody (human IgG) gave negative staining. #37, #55, and the control antibody were not reactive with uninfected Huh7.5 cells.
doi:10.1371/journal.pone.0055874.g004

These two fractions were further examined by the FFU assay for their infectivity titers. Fractions 3 and 6 had an infectivity titer of 2.0×10^4 FFU/0.1 ml and 4.7×10^3 FFU/0.1 ml, respectively. Fraction 3 was calculated to have an approximately 9 times higher infectivity titer per HCV RNA than fraction 6 (**Figure 5B**), which was in accordance with our previous observation that the fraction with lower buoyant density was more infectious [25]. Thus, we selected fraction 3 for the EM examination. Fraction 3 was treated with #37 followed by anti-human IgG labeled with colloidal gold-particles, negatively stained, and examined in a transmission electron microscope. We detected HCV-like particles coated with colloidal gold, indicating the binding of #37 to virions. Most of the viral particles reacting with #37 measured approximately 50–60 nm in diameter. **Figure 5C (a)** shows an aggregate of three virions coated with specific gold. These viral particles measured approximately 50 nm in diameter. **Figure 5C (b)** shows two particles; the one on the right (50-nm in diameter) was coated with colloidal gold, indicating the binding of #37. Another particle on the left (35-nm in diameter) was negative for colloidal gold, indicating that #37 was not reactive with this particle. In addition, the presence of such uncoated particle in the same field suggested that colloidal gold did not bind non-specifically. When fraction 3 was reacted with #55 followed by anti-human IgG labeled with colloidal gold particles, larger aggregates of various-sized viral particles were observed, as shown in **Figure 5C (c)**. The viral particles varied in sizes from 40 to 70 nm in diameter. Immuno-gold EM demonstrated that both #37 and #55 can bind to HCV particles. **Figure 5C (d)** shows negative reaction of colloidal gold by an irrelevant control antibody (human IgG).

Neutralizing Activity

To investigate whether #37 and #55 could inhibit HCV infection, we performed an *in vitro* neutralization assay by reduction of FFU. As HCV inocula, we used chimeric H77/C3 (genotype 1a), chimeric Con1/C3 (genotype 1b), and chimeric J6/C3 (genotype 2a) in this assay. A virus sample containing approximately 300 FFU/ml of HCV was pretreated at 4°C overnight with #37, #55, or an irrelevant control antibody at a final concentration of 0.1, 0.5, 2.5, 12.5, 62.5, or 312.5 μg/ml and the mixtures were then inoculated into Huh7.5 cells. After 48 h post-infection, IF-positive foci were manually counted under a fluorescence microscope. Each test was performed in duplicate. As shown in **Figure 6**, compared to the results obtained with an irrelevant control antibody, #55 inhibited the viral infection in dose-dependent manner for all of the 3 samples tested. Inhibition by #37 was not observed.

Since #55 was found to have a neutralizing activity as shown above, further examination by the FFU reduction assay was conducted with HCV strain JFH1 (genotype 2) and various chimeric HCV containing the E2 proteins from 9 different genotypes. Chimeric viruses tested included H77C/JFH1 (genotype 1a), J4/JFH1 (genotype 1b), J6/JFH1 (genotype 2a), J8/JFH1 (genotype 2b), S52/JFH1 (genotype 3a), ED43/JFH1 (genotype 4a), SA13/JFH1 (genotype 5a), HK6a/JFH1 (genotype 6a), and QC69/JFH1 (genotype 7a). Two different concentrations of target

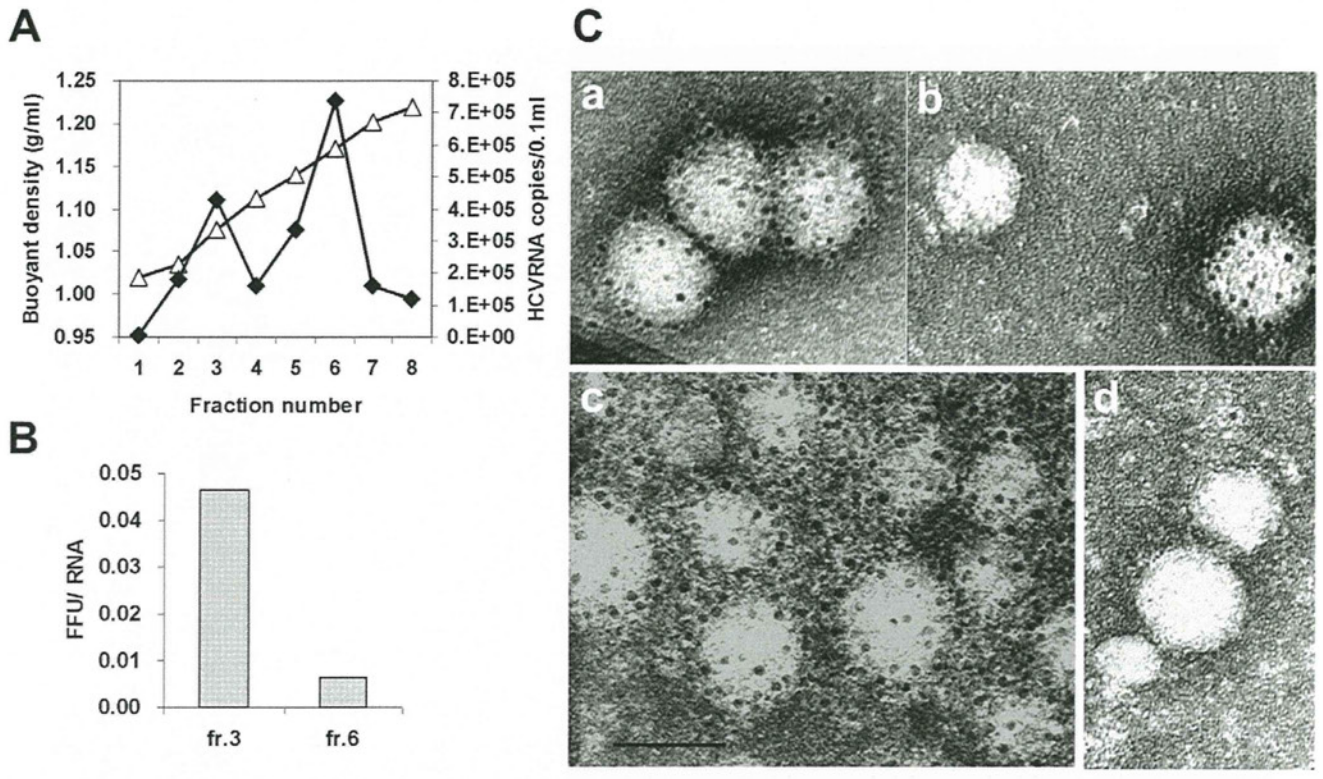

Figure 5. Immuno-gold EM demonstrated that both #37 and #55 recognized HCV intact particles. (**A**). Equilibrium SDG centrifugation. ◆, HCV RNA copies measured by RT-qPCR; Δ, buoyant densities. (**B**). The ratio of infectivity titer (FFU) to HCV RNA copies of fractions 3 and 6. (**C**). Immuno-gold EM. Viral particles in fraction 3 were treated with #37 (**a, b**), #55 (**c**), or a control antibody (**d**) followed by anti-human IgG conjugated with colloidal gold particles, and examined under an electron microscope. HCV-like particles in the sample treated with #37 and #55 were observed with specific labeling of gold particles indicating that the antibodies are capable of binding to viral particles. Bar = 50 nm.
doi:10.1371/journal.pone.0055874.g005

HCV were tested in the assays. The one virus-sample contained 10^2 FFU/0.1 ml (no.1) and another 10^3 FFU/0.1 ml (no.2). **Table 2** shows the 50% neutralization titers (NT_{50}) of #55, a lowest concentration (μg/ml) required for 50% reduction of FFU, calculated by curvilinear regression analysis. #55 neutralized HCV infection of various genotypes (1a, 1b, 2a, 3a, 4a, 5a, and 6a), with the NT_{50} titers ranging from 2 to 127 μg/ml for no.1 and 6 to 231 μg/ml for no.2. Neutralization of genotype 7a (QC69/JFH1) by #55 was less, with a NT_{50} titer of 219 μg/ml for no.1 and >500 μg/ml for no.2.

Blocking of Viral Adsorption

We examined whether #55 blocked viral adsorption to cells by measuring the amount of cell-attached HCV RNA using RT-qPCR. A half ml of the culture supernatant containing 10^5 FFU/ml of chimeric HCV, H77/C3, was pre-treated at 4°C for 24 h with an equal volume of #55, #37 or a control antibody at a final

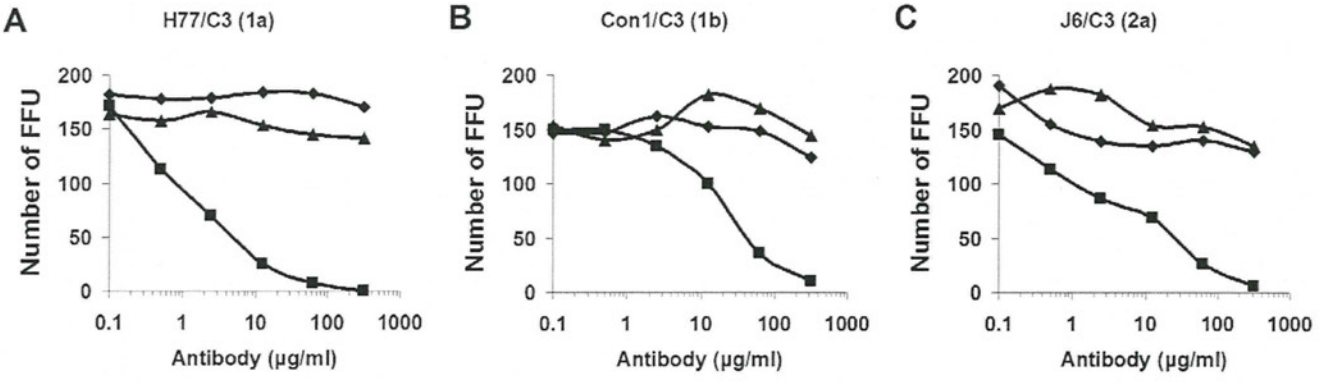

Figure 6. Neutralization assay by FFU reduction. The mean numbers of positive foci are shown for viruses H77/C3 (**A**), Con1/C3 (**B**), and J6/C3 (**C**). Compared to the results obtained with an irrelevant control antibody, #55 inhibited the viral infection in dose-dependent manner for all of the 3 samples tested. Inhibition by #37 was not observed. ◆, control; ■, #55; ▲, #37.
doi:10.1371/journal.pone.0055874.g006

Table 2. 50% neutralization titers (NT_{50}) of #55 by FFU reduction.

Virus (genotype)	NT_{50} (μg/ml)*	
	no.1	no.2
H77C/JFH1 (1a)	10.6	10.3
J4/JFH1 (1b)	ND	9.3
J6/JFH1 (2a)	126.6	99.1
J8/JFH1 (2b)	21.1	24.1
S52/JFH1 (3a)	73.0	230.8
ED43/JFH1 (4a)	1.3	7.4
SA13/JFH1 (5a)	5.0	5.7
HK6a/JFH1 (6a)	5.2	7.3
QC69/JFH1 (7a)	218.5	>500
JFH1 (2a)	2.0	ND

*, calculated by curvilinear regression analysis; ND, not done.
doi:10.1371/journal.pone.0055874.t002

concentration of 500, 50, or 5 μg/ml. The mixtures were then inoculated onto Huh7.5 cells seeded in 12-well plates (5×10^5 cells/well). After incubation for 4 h at 37°C, cells were washed 3 times with PBS. Amount of cell-associated HCV RNA in a well was measured by RT-qPCR. Each test was performed in duplicate. Compared to the control antibody (human IgG), #55 inhibited viral adsorption in dose-dependent manner, as shown in **Figure 7**. Inhibition by #37 was not observed but rather slightly enhanced at a concentration of 50 μg/ml.

Specific amino acids (W420, Y527, W529, G530, and D535) in the E2 envelope protein of HCV were reported to be critical for binding to CD81, a principal cellular receptor and they were conserved across all genotypes [26]. As the epitope of #55 includes these amino acid residues, it was possible that #55 blocked virus adsorption by competing with CD81 for a binding site on the E2 envelope. **Figure 8A** shows sequence alignment of aa 508 to 607, the epitope of #55, of HCV employed in the present study. The epitope of #55 contains the residues important for binding to CD81 (asterisks). Thus, we investigated this possibility by testing whether CD81 inhibits binding of HCV to #55 utilizing an assay based on antibody-captured RT-qPCR. A

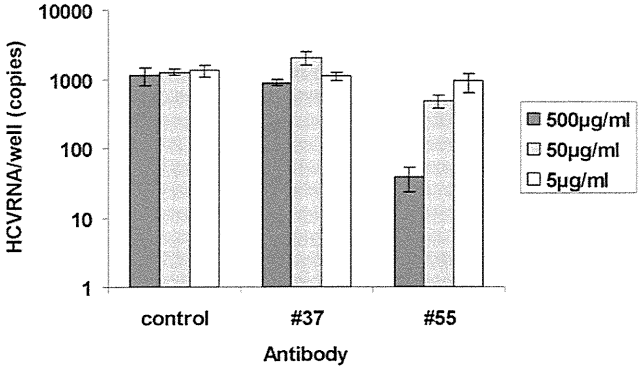

Figure 7. Blocking of viral adsorption by #55. Blocking of viral adsorption measured by RT-qPCR. Compared to the control antibody (human IgG), #55 inhibited viral adsorption in dose-dependent manner. Inhibition by #37 was not observed but rather slightly enhanced at a concentration of 50 μg/ml.
doi:10.1371/journal.pone.0055874.g007

100 μl of the virus solution containing 10^4 FFU/ml of H77/C3 was incubated with an equal volume of various dilutions of soluble recombinant human CD81 protein (Origene, Rockville, MD, USA) for 2 h at room temperature. Each mixture was then inoculated into a 48-well plate which was pre-coated with #55 or an irrelevant control antibody (human IgG) at a concentration of 10 μg/ml. The plate was incubated at 4°C overnight. After washing, bound HCV RNA was extracted and quantified by RT-qPCR. As shown in **Figure 8B**, CD81 inhibited the binding of virus to #55 in a dose-dependent manner.

Discussion

In this study, as an approach to obtain human B cell lines producing antibodies to HCV envelope E2, we applied the EBV transformation method, which is based on the fact that EBV transforms B-lymphocytes of humans *in vitro* into lymphoblastoid cells that synthesize and secrete immunoglobulins. From PBMC collected from a patient persistently infected with HCV strain H (genotype 1a) we have successfully isolated two clones producing anti-HCV E2 antibodies, #37 and #55. At the first screening of culture supernatants, several wells of a 96-well plate were found positive for anti-HCV E2 antibodies. However, most of them became negative as further cultured. Finally #37 and #55 remained as stably producing clones.

There was remarkable contrast between these two antibodies in their properties: (1) #55 appeared to be a broadly cross-neutralizing antibody. In the neutralization assay by FFU reduction, it inhibited infection by HCV genotypes 1a, 1b, 2a, 2b, 3a, 4a, 5a, 6a, and, to a lesser extent, 7a. In contrast, #37 did not neutralize any of the viruses tested. Interestingly it tended to enhance the infection at low concentrations (**Figure 6B and C,** and **Figure 7**): (2) the epitope of #55 was mapped to the region of aa 508 to 607 and that of #37 was mapped to the longer region spanning aa 429 to 652 of the E2 protein. #55 seemed unique for broadly cross-neutralizing antibody to have a relatively short conformational epitope, since it has been reported that conformational epitopes reacting with such antibodies are usually retained in the full length E2 [7,9]: (3) when we tested their cross-reactivity using transfected Huh7 cells expressing the E2 proteins, #37 was reactive with genotype 1a but reacted very weakly with the others, while #55 was broadly reactive with all genotypes tested. However, when examined using the virus-infected cells as targets, #37 was reactive with all HCV genotypes tested, although its binding activity measured by IF was less than that of #55 except for H77C/JFH1(1a) and S52/JFH(3a): (4) in immuno-gold EM, viral particles recognized by #37 were rather homogenous in size and measured approximately 50–60 nm in diameter. On the other hand, #55 produced larger aggregates of various-sized viral particles, probably because of its higher binding activity: (5) the antibodies showed a different pattern of IF-staining in the HCV-infected cells. While #37 gave granular reactions mostly in the periphery of nuclei, #55 gave diffuse staining throughout the cytoplasm (**Figure 4**). The nature of the antigens reacting with #37 and #55 remains to be studied.

Recently, Keck et al. reported that the region aa 529 to 535 of the E2 envelope protein is a CD81 binding region that does not tolerate neutralization escape mutations [27]. The epitope of #55 includes the above mentioned region and #55 blocked virus adsorption by competing with CD 81 for a binding site on the E2 envelope. As #55 is broadly neutralization cross-reactive, it may be very useful in preventing infection by HCV of various genotypes. Sasayama et al. reported that blocking N-glycosylation of aa 534 (aa 532 of strain H77) in this region by substituting

A

```
                    508         • • • ••   •             552                                                  607   References
H77/C3(1a)          CFTPSPVVVGTTDRSGAPTYSWGANDTDVFVLNNTRPPLGNWFGCTWMNSTGFTKVCGAPPCVI.GGVGNNT....LLCPTDCFPKHPEATYSRCGSGPWITPRC  [17]
Con1/C3(1b)         --------------F-V------E-E---LL-------Q----------------T--G---N-.--I--K-....-T------R-------TK------L----  [17]
J6/C3(2a)           --------------L-----T--E-E----L--S------S--------------T------RT.RADFNASTD..--------R---DT--LK------L----  [17]
JFH1(2a)            --------------R-V---T--E-E----L--S----Q-S---------S-Y--T------RT.RADFNASTD..--------R---D---IK------L--K-  [5]
H77C/JFH1(1a)       ---------------------------------------------------------------.-------....--------R-------------------  [20]
J4/JFH1(1b)         ----------------V------E-E---ML-------Q----------------T--G---N-.-----R-....-I------R-------TK------L----  [18]
J6/JFH1(2a)         --------------L-----T--E-E----L--S------S---------S-Y--T------RT.RADFNASTD..--------R---DT--LK------L----  [19]
J8/JFH1(2b)         -------------KQ-V---T--E-E----L--S----R-A--------G-----T------R-.RKDY-S-ID..--------R---D---LK--A---L----  [18]
S52/JFH1(3a)        -------------IK-K---N--E-E----L-ESL---S-R----A-------L-T------N-Y--E-DPENETD-F------R-----------A---L----  [22]
ED43/JFH1(4a)       -------------HV-V---T--E-E----L--S----H-A----V---------T------EV.NTNNGT.....WH------R----T--AK----------  [20]
SA13/JFH1(5a)       --------------K-N------E-E--I-L-------T-------------V-T------NL.-PT---S.....K------R---D---TK------L----  [21]
HK6a/JFH1(6a)       -------------KL-I---N--E-E----M-ESL---T-G--------------T------Q-.VPGDY-SSANE--------R-------Q-----------  [18]
QC69/JFH1(7a)       --------------R-V---T--E-ES---L--S----Q-S----S---T-----T--G---K-.RPQ-AQSNTS.-T------R---R----A------L----  [18]
```

☆, important amino acids for binding to CD81[26]

B

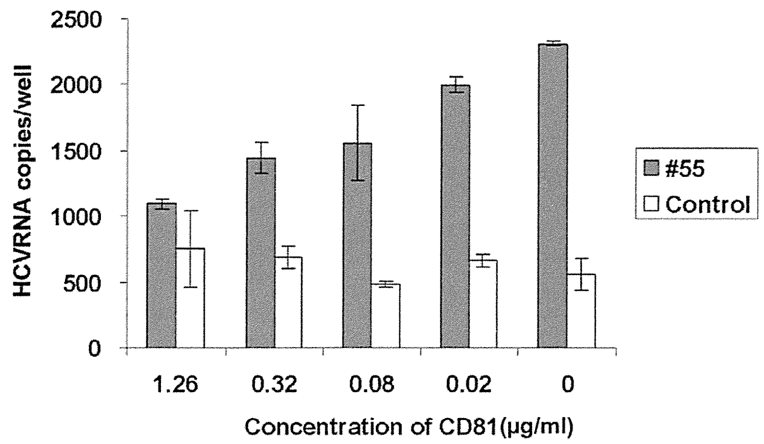

Figure 8. Binding of HCV to #55 was inhibited by soluble recombinant CD81. (**A**). Sequence alignment of aa 508 to 607, the epitope of #55, of various genotypes of HCV employed in the present study. Residues identical to the sequences of H77/C3 are indicated by a dash. Dots indicate gaps. (**B**). H77/C3 virus was treated with various dilutions of soluble CD81.The mixtures were inoculated into a 48-well plate that was pre-coated with #55 or the control antibody. Amount of bound HCV RNA was measured by RT-qPCR.
doi:10.1371/journal.pone.0055874.g008

asparagine with histidine markedly enhanced the sensitivity of the virus to neutralizing antibodies and suggested that the aa 529 to 535 region is usually protected from the antibody's access by the N-glycosylation [28]. It is possible that #55 may evade the N-glycosylation mediated protective mechanism of HCV.

A cross-neutralizing monoclonal antibody that could be generated in large volume might be particularly beneficial to prevent the almost universal occurrence of HCV re-infection of transplanted livers and could play other roles in immunoprophylaxis until such time as an effective HCV vaccine is developed and commercialized.

Acknowledgments

We thank Mari Komoto (Kobe University, Kobe, Japan) for technical assistance.

Author Contributions

Conceived and designed the experiments: YKS RHP. Performed the experiments: YKS MH MO. Analyzed the data: YKS KS HY HH. Contributed reagents/materials/analysis tools: HJA. Wrote the paper: YKS RHP HJA HY.

References

1. Shimizu YK, Hijikata M, Iwamoto A, Alter HJ, Purcell RH, et al. (1994) Neutralizing antibodies against hepatitis C virus and the emergence of neutralization escape mutant viruses. J Virol 68: 1494–1500.
2. Logvinoff C, Major ME, Oldash D, Heyward S, Talal A, et al. (2004) Neutralizing antibody response during acute and chronic hepatitis C virus infection. Proc Natl Acad Sci U S A 101: 10149–10154.
3. Ishii K, Rosa D, Watanabe Y, Katayama T, Harada H, et al. (1998) High titers of antibodies inhibiting the binding of envelope to human cells correlate with natural resolution of chronic hepatitis C. Hepatology 28: 1117–1120.
4. Farci P, Alter HJ, Wong DC, Miller RH, Govindarajan S, et al. (1996) Prevention of hepatitis C virus infection in chimpanzees by hyperimmune serum against the hypervariable region 1 of the envelope 2 protein. Proc Natl Acad Sci U S A 93: 15394–15399.
5. Wakita T, Pietschmann T, Kato T, Date T, Miyamoto M, et al. (2005) Production of infectious hepatitis C virus in tissue culture from a cloned viral genome. Nat Med 11: 791–796.
6. Meunier JC, Russell RS, Goossens V, Priem S, Walter H, et al. (2008) Isolation and characterization of broadly neutralizing human monoclonal antibodies to the E1 glycoprotein of hepatitis C virus. J Virol 82: 966–973.
7. Perotti M, Mancini N, Diotti RA, Tarr AW, Ball JK, et al. (2008) Identification of a broadly cross reacting and neutralizing human monoclonal antibody directed against the hepatitis C virus E2 protein. J Virol 82: 1047–1052.
8. Owsianka AM, Tarr AW, Keck ZY, Li TK, Witteveldt J, et al. (2008) Broadly neutralizing human monoclonal antibodies to the hepatitis C virus E2 glycoprotein. J Gen Virol 89: 653–659.

9. Mancini N, Diotti BA, Perotti M, Sautto G, Clementi N, et al. (2009) Hepatitis C virus (HCV) infection may elicit neutralizing antibodies targeting epitopes conserved in all viral genotypes. PLoS ONS 4: 1–7.
10. Broering TJ, Garrity KA, Boatright NK, Sloan SE, Sandor F, et al. (2009) Identification and Characterization of broadly neutralizing human monoclonal antibodies directed against the E2 envelope glycoprotein of hepatitis C virus. J Virol 83: 12473–12482.
11. Giang E, Dorner M, Prentoe JC, Dreux M, Evans MJ, et al. (2012) Human broadly neutralizing antibodies to the envelope glycoprotein complex of hepatitis C virus. Proc Natl Acad Sci U S A 109: 6205–6210.
12. Feinstone SM, Alter HJ, Dienes P, Shimizu Y, Popper H, et al. (1981) Non-A, non-B hepatitis in chimpanzees and marmosets. J Infect Dis 144: 588–597.
13. Blight KJ, Mckeating JA, Rice CM (2002) Highly permissive cell lines for subgenomic and genomic hepatitis C virus. J Virol 76: 13001–13014.
14. Shimizu YK, Purcell RH, Yoshikura H (1993) Correlation between the infectivity of hepatitis C virus in vivo and its infectivity in vitro. Proc Natl Acad Sci U S A 90: 6037–6041.
15. Shimizu YK, Hijikata M, Oshima M, Shimizu K, Yoshikura H (2006) Detection of a 5′ end subgenome of hepatitis C virus terminating at nucleotide 384 in patients' plasma and liver tissues. J Viral Hepatitis 13: 746–755.
16. Forns X, Allander T, Rohwer-Nutter P, Bukh J (2000) Characterization of modified hepatitis C virus E2 proteins expressed on the cell surface. Virology 274: 75–85.
17. Pietschmann T, Kaul A, Koutsoudakis G, Shavinskaya A, Kallis AS, et al. (2006) Construction and characterization of infectious intragenotypic and intergenotypic hepatitis C chimeras. Proc Natl Acad Sci U S A 103: 7408–7413.
18. Gottwein JM, Scheel TK, Jensen TB, Lademann JB, Prentoe JC, et al. (2009) Development and characterization of hepatitis C virus genotype 1–7 cell culture systems: role of CD81 and Scavenger Receptor Class B type 1 and effect of antiviral drugs. Hepatology 49: 364–377.
19. Yi-Ping L, Gottwein JM, Scheel TK, Jensen TB, Bukh J (2011) MicroRNA-122 antagonism against hepatitis C virus genotypes1–6 and reduced efficacy by host RNA insertion or mutations in the HCV 5′ UTR. Proc Natl Acad Sci U S A 108: 4991–4996.
20. Scheel TK, Gottwein JM, Jensen TB, Prentoe JC, Hoegh AM, et al. (2008) Development of JFH1-based cell culture systems for hepatitis C virus genotype 4a and evidence for cross-genotype neutralization. Proc Natl Acad Sci U S A 105: 997–1002.
21. Jensen TB, Gottwein JM, Scheel TK, Hoegh AM, Eugen-Olsen J, et al. (2008) Highly efficient JFH1-based cell culture system for hepatitis C virus genotype 5a: Failure of homologous neutralization-antibody treatment to control infection. J Infect Dis 198: 1756–1765.
22. Gottwein JM, Scheel TK, Hoegh AM, Lademann JB, Eugen-Olsen J, et al. (2007) Robust hepatitis C genotype 3a cell culture releasing adapted intergenotypic 3a/2a (S52/JFH1) viruses. Gastroenterology 133: 1614–1624.
23. Shimizu YK, Oomura M, Abe K, Uno M, Yamada E, et al. (1985) Production of antibody associated with non-A, non-B hepatitis in a chimpanzee lymphoblastoid cell line established by in vitro transformation with Epstein-Barr virus. Proc Natl Acad Sci U S A 82: 2138–2142.
24. Gastaminza P, Dryden K, Boyd B, Wood M, Law M, et al. (2010) Ultrastructural and biophysical characterization of hepatitis C virus particles produced in cell culture. J Virol 84: 10999–11009.
25. Hijikata M, Shimizu YK, Kato H, Iwamoto A, Shih JW, et al. (1993) Equilibrium centrifugation studies of hepatitis C virus: Evidence for circulating immune complexes. J Virol 67: 1953–1958.
26. Owsianka AM, Timms JM, Tarr AW, Brown JP, Hickling TP, et al. (2006) Identification of conserved residues in the E2 glycoprotein of the hepatitis C virus that are critical for CD81 binding. J Virol 80: 8695–8704.
27. Keck ZY, Saha A, Xia J, Wang Y, Lau P, et al. (2011) Mapping a region of hepatitis C virus E2 that is responsible for escape from neutralizing antibodies and a core CD81-binding region that does not tolerate neutralization escape mutations. J Virol 85: 10451–10463.
28. Sasayama M, Shoji I, Adianti M, Jiang DP, Deng L, et al. (2012) A point mutation at asn-534 that disrupts a conserved N-glycosylation motif of the E2 glycoprotein of hepatitis C virus markedly enhances the sensitivity to antibody neutralization. J Med Virol 84: 229–234.

HEPATOLOGY
Official Journal of the American Association for the Study of Liver Diseases

Hepatitis C Virus NS4B Protein Targets STING and Abrogates RIG-I–Mediated Type I Interferon-Dependent Innate Immunity

Sayuri Nitta,[1*] Naoya Sakamoto,[1,2,6*] Mina Nakagawa,[1,2] Sei Kakinuma,[1,2] Kako Mishima,[1] Akiko Kusano-Kitazume,[1] Kei Kiyohashi,[1] Miyako Murakawa,[1] Yuki Nishimura-Sakurai,[1] Seishin Azuma,[1] Megumi Tasaka-Fujita,[1] Yasuhiro Asahina,[1,2] Mitsutoshi Yoneyama,[3] Takashi Fujita,[4,5] and Mamoru Watanabe[1]

Hepatitis C virus (HCV) infection blocks cellular interferon (IFN)-mediated antiviral signaling through cleavage of Cardif by HCV-NS3/4A serine protease. Like NS3/4A, NS4B protein strongly blocks IFN-β production signaling mediated by retinoic acid–inducible gene I (RIG-I); however, the underlying molecular mechanisms are not well understood. Recently, the stimulator of interferon genes (STING) was identified as an activator of RIG-I signaling. STING possesses a structural homology domain with flaviviral NS4B, which suggests a direct protein-protein interaction. In the present study, we investigated the molecular mechanisms by which NS4B targets RIG-I–induced and STING-mediated IFN-β production signaling. IFN-β promoter reporter assay showed that IFN-β promoter activation induced by RIG-I or Cardif was significantly suppressed by both NS4B and NS3/4A, whereas STING-induced IFN-β activation was suppressed by NS4B but not by NS3/4A, suggesting that NS4B had a distinct point of interaction. Immunostaining showed that STING colocalized with NS4B in the endoplasmic reticulum. Immunoprecipitation and bimolecular fluorescence complementation (BiFC) assays demonstrated that NS4B specifically bound STING. Intriguingly, NS4B expression blocked the protein interaction between STING and Cardif, which is required for robust IFN-β activation. NS4B truncation assays showed that its N terminus, containing the STING homology domain, was necessary for the suppression of IFN-β promoter activation. NS4B suppressed residual IFN-β activation by an NS3/4A-cleaved Cardif (Cardif1-508), suggesting that NS3/4A and NS4B may cooperate in the blockade of IFN-β production. *Conclusion*: NS4B suppresses RIG-I–mediated IFN-β production signaling through a direct protein interaction with STING. Disruption of that interaction may restore cellular antiviral responses and may constitute a novel therapeutic strategy for the eradication of HCV. (HEPATOLOGY 2013;57:46-58)

Type I interferon (IFN) plays a central role in eliminating hepatitis C virus (HCV) both under physiological conditions and when used as a therapeutic intervention.[1-3] In experimental acute-resolving HCV infection in chimpanzees, numerous IFN-related genes are expressed during clinical course of infection.[4] Viruses are recognized by cellular innate immune receptors, such as toll-like receptors, and a family of RIG-I–like receptors, such as retinoic-acid-inducible gene I (RIG-I) and melanoma-differentiation-associated gene 5 (MDA-5); host antiviral responses are then activated, resulting in the

From the [1]Departments of Gastroenterology and Hepatology; [2]Departments of Hepatitis Control, Tokyo Medical and Dental University, Tokyo, Japan; [3]Division of Molecular Immunology, Medical Mycology Research Center, Chiba University, Chiba, Japan; [4]Laboratory of Molecular Genetics, Department of Genetics and Molecular Biology, Institute for Virus Research, Kyoto University, Kyoto, Japan; [5]Laboratory of Molecular Cell Biology, Graduate School of Biostudies, Kyoto University, Kyoto, Japan; and [6]Department of Gastroenterology and Hepatology, Hokkaido University, Hokkaido, Japan.

Received September 16, 2011; accepted July 24, 2012.

BiFC, bimolecular fluorescence complementation; CARD, caspase recruitment domain; DAPI, 4',6-diamidino-2-phenylindole; dsRNA, double-stranded RNA; ER, endoplasmic reticulum; FACL4, fatty acid-CoA ligase, long chain 4; HCV, hepatitis C virus; IFN, interferon; IKKε, IκB kinase ε; IRF-3, interferon-regulatory factor 3; ISRE, interferon-stimulated response element; MAM, mitochondria-associated ER membrane; mKG, monomeric Kusabira-Green; PDI, protein disulphide-isomerase; pIRF-3, phosphorylated IRF3; poly(dA:dT), poly(deoxyadenylic-deoxythymidylic) acid; RIG-I, retinoic acid–inducible gene I; siRNA, small interfering RNA; SOCS, suppressor of cytokine signaling; STAT1, signal transducer and activator of transcription protein-1; STING, stimulator of interferon genes; TBK1, TANK binding kinase 1.

**These authors contributed equally to this work.*

production of cytokines such as type I and type III IFNs.[5] RIG-I is activated through recognition of short double-strand RNA (dsRNA) or triphosphate at the 5′ end of dsRNA as pathogen-associated molecular patterns,[6,7] forming a homo-oligomer that binds with the caspase recruitment domain (CARD) of Cardif (also known as MAVS, VISA, or IPS-1).[8-11] Cardif subsequently recruits TANK binding kinase 1 (TBK1) and IκB kinase ϵ (IKKϵ) kinases, which catalyze phosphorylation and activation of IFN regulatory factor-3 (IRF-3).[12] Activation of TBK1 and IKKϵ results in the phosphorylation of IRF-3 or IRF-7, translocation to the nucleus, and induction of IFN-β mRNA transcription.

Several HCV proteins can block host cellular antiviral responses. HCV core protein blocks IFN signaling by interacting with signal transducer and activator of transcription protein-1 (STAT1).[13] The core protein also induces expression of suppressor of cytokine signaling-1 (SOCS1) and SOCS3, and blocks Janus kinase–STAT signaling.[14,15] A well-elucidated immune evasion strategy of HCV involves NS3/4A serine protease and its ability to inhibit host IFN signal pathways. Gale and colleagues[11,16,17] revealed that NS3/4A protease cleaves Cardif at Cys-508 resulting in dislocation of Cardif from mitochondria, and blocks downstream signaling of IFN-β production. On the other hand, Baril et al.[18] reported that Cardif was still able to form a homo-oligomer and to activate downstream IFN production signaling despite delocalization from the mitochondria. These reports suggest that homo-oligomerization of Cardif, and not mitochondrial anchorage, is essential for the activation of downstream IFN signaling and that other virus-derived molecules may cooperate with NS3/4A to abrogate the signaling of IFN production.

We reported previously that HCV-NS4B, as well as NS3/4A, inhibited RIG-I and Cardif-mediated interferon-stimulated response element (ISRE) activation, while TBK1- and IKKϵ-mediated ISRE activation were not suppressed.[19] These results indicate that NS4B suppresses IFN production signaling by targeting Cardif or other unknown signaling molecules between the level of Cardif and TBK1/IKKϵ.

Recently, a stimulator of interferon genes (STING, also known as MITA/ERIS/MPYS/TMEM173) was identified as a positive regulator of RIG-I–mediated IFN-β signaling.[20-23] STING is a 42-kDa protein localized predominantly in the endoplasmic reticulum (ER) that binds RIG-I, Cardif, TBK1, and IKKϵ. STING is thought to act as a scaffold for Cardif/TBK1/IRF-3 complex upon viral infection.[22] It has been reported that NS4B of yellow fever virus, which is a member of the flaviviridae family of viruses, inhibits STING activation probably through a direct molecular interaction.[24] These reports have led us postulate that HCV-NS4B may also inhibit RIG-I dependent IFN signaling through association with STING.

In the present study, we further investigated the molecular mechanisms by which HCV-NS4B protein inhibits RIG-I–mediated IFN expression signaling. We demonstrated that HCV-NS4B specifically binds STING, blocks the molecular interaction between STING and Cardif, and suppresses the RIG-I–like receptor–induced activation of IFN-β production signaling.

Materials and Methods

Plasmids. The ΔRIG-I and RIG-IKA plasmids express constitutively active and inactive RIG-I, respectively.[5] Full-length Cardif (Cardif) and CARD-truncated Cardif (ΔCARD) plasmids were provided by J. Tschopp.[11] Plasmids expressing STING were provided by G. N. Barber.[20] Plasmids expressing HCV NS3/4A, NS4B, and truncated NS4B have been described.[25] Plasmid pIFNβ-Fluc was provided by R. Lin.[26]

Cell Culture. HEK293T and Huh7 cells were maintained in Dulbecco's modified minimal essential medium (Sigma) supplemented with 2 mM L-glutamine and 10% fetal calf serum at 37°C with 5% CO_2.

HCV Replicon Constructs and HCV-JFH1 Cell Culture. An HCV subgenomic replicon plasmid, pRep-Feo, expressed fusion protein of firefly luciferase and neomycin phosphotransferase.[27,28] Huh7 cells were transfected by Rep-Feo RNA, cultured in the presence of 500 μg/mL of G418, and a cell line that stably expressed Feo replicon was established. For HCV cell culture, the HCV-JFH1 strain was used.[29,30]

Antibodies. Antibodies used were anti–IRF-3 (FL-425, Santa Cruz Biotechnology), anti-HA (Invitrogen), anti-myc (Invitrogen), mouse anti-PDI (Abcam),

Address reprint requests to: Naoya Sakamoto, M.D., Ph.D., Department of Gastroenterology and Hepatology, Hokkaido University, Kita15, Nishi8, Kita-ku, Sapporo, Hokkaido, 060-0808, Japan. E-mail: nsakamoto.gast@rmd.ac.jp; fax (81)-11-706-8036.

View this article online at wileyonlinelibrary.com.

DOI 10.1002/hep.26017

Potential conflict of interest: Nothing to report.

Additional Supporting Information may be found in the online version of this article.

rabbit anti-PDI (Enzo Life Science), anti-Flag (Sigma Aldrich), anti-Cardif (Enzo Life Science), anti-phospho–IRF-3 (Ser396, Millipore), anti-monomeric Kusabira-Green C- or N-terminal fragment (MBL), and anti-FACL4 (Abgent).

Luciferase Reporter Assay. IFN-β reporter assays were performed as described.[19,31] The plasmids pIFN-β-Fluc and pRL-CMV were cotransfected with NS3/4A or NS4B, and ΔRIG-I, Cardif, STING or poly(deoxyadenylic-deoxythymidylic) acid [poly(dA:dT)] (Invivogen). RIG-IKA, ΔCARD, and pcDNA3.1, respectively, were used as controls. Luciferase assays were performed 24 hours after transfection by using a 1420 Multilabel Counter (ARVO MX PerkinElmer) and Dual Luciferase Assay System (Promega). Assays were performed in triplicate, and the results are expressed as the mean ± SD.

Immunoblotting. Preparation of total cell lysates was performed as described.[19,28] Protein was separated using NuPAGE 4%-12% Bis/Tris gels (Invitrogen) and blotted onto an Immobilon polyvinylidene difluoride membrane. The membrane was immunoblotted with primary followed by secondary antibody, and protein was detected by chemiluminescence.

Immunoprecipitation Assay. HEK-293T or Huh7 cells were transfected with plasmids as indicated. Twenty-four hours after transfection, cellular proteins were harvested and immunoprecipitation assays were performed using an Immunoprecipitation Kit according to the manufacturer's protocol (Roche Applied Science). The immunoprecipitated proteins were analyzed by immunoblotting.

Indirect Immunofluorescence Assay. Cells seeded onto tissue culture chamber slides were transfected with plasmids as indicated. Twenty-four hours after transfection, the cells were fixed with cold acetone and incubated with primary antibody and subsequently with Alexa488- or Alexa568-labeled secondary antibodies. Mitochondria were stained by MitoTracker (Invitrogen). Cells were visualized using a confocal laser microscope (Fluoview FV10, Olympus).

BiFC Assay. Expression plasmids of NS4B, Cardif, or STING that was fused with N- or C-terminally truncated monomeric Kusabira-Green (mKG) were constructed by inserting polymerase chain reaction–amplified fragments encoding NS4B, Cardif, or STING, respectively, inserted into fragmented mKG vector (Coral Hue Fluo-Chase Kit; MBL). HEK293T cells were transfected with a complementary pair of mKG fusion plasmids. Twenty-four hours after transfection, fluorescence-positive cells were detected and counted by flow cytometry, or observed by confocal laser microscopy.

Small Interfering RNA Assay. Nucleotide sequences of STING-targeted small interfering RNAs (siRNAs) were as follows: (1) 5′-gcaacagcatctatgagcttctggagaac-3′, (2) 5′- gtgcagtgagccagcggctgtatattctc;-3′, (3) 5′-gctggcat ggtcatattacatcggatatc-3′.[22] Stealth RNAi Negative Control Duplex (Medium GC Duplex, Invitrogen) was used. Forty-eight hours after siRNA transfection, expression levels of STING were detected by immunoblotting.

Statistical Analyses. Statistical analyses were performed using unpaired, two-tailed Student t test. $P < 0.05$ were considered to be statistically significant.

Results

NS4B Suppressed RIG-I, Cardif, and STING-Mediated Activation of IFN-β Expression Signaling. First, we performed a reporter assay using a luciferase reporter plasmid regulated by native IFN-β promoter. Consistent with our previous study,[19] overexpression of NS4B, as well as NS3/4A, inhibited the IFN-β promoter activation that was induced by ΔRIG-I and Cardif, respectively (Fig. 1A). We next studied whether NS4B targets STING and inhibits RIG-I pathway–mediated activation of IFN-β production. Expression of NS4B protein significantly suppressed STING-mediated activation of the IFN-β promoter reporter, whereas expression of NS3/4A showed no effect on STING-induced IFN-β promoter activity (Fig. 1A). To study whether NS4B blocks the STING-mediated DNA-sensing pathway, we performed a reporter assay using a luciferase reporter plasmid cotransfection with poly(dA:dT), which is a synthetic analog of B-DNA and has been reported to induce STING-mediated IFN-β production and NS4B. NS4B significantly blocked poly(dA:dT)-induced IFN-β promoter activation, suggesting that NS4B may block STING signaling in the DNA-sensing pathway (Fig. 1A).

Activation of RIG-I signaling induces phosphorylation of IRF-3, which is a hallmark of IRF-3 activation.[32] Thus, we examined the effects of NS3/4A and NS4B expression on phosphorylation of IRF-3 by immunoblotting analysis. As shown in Fig. 1B, overexpression of ΔRIG-I, Cardif, or STING in HEK293T cells increased levels of phosphorylated IRF-3 (pIRF-3). Expression of NS4B impaired the IRF-3 phosphorylation that was induced by ΔRIG-I, Cardif, or STING. NS3/4A also blocked production of pIRF-3 induced by ΔRIG-I or Cardif. Intriguingly, NS3/4A did not block STING-induced pIRF-3 production. These results demonstrate that both NS3/4A and

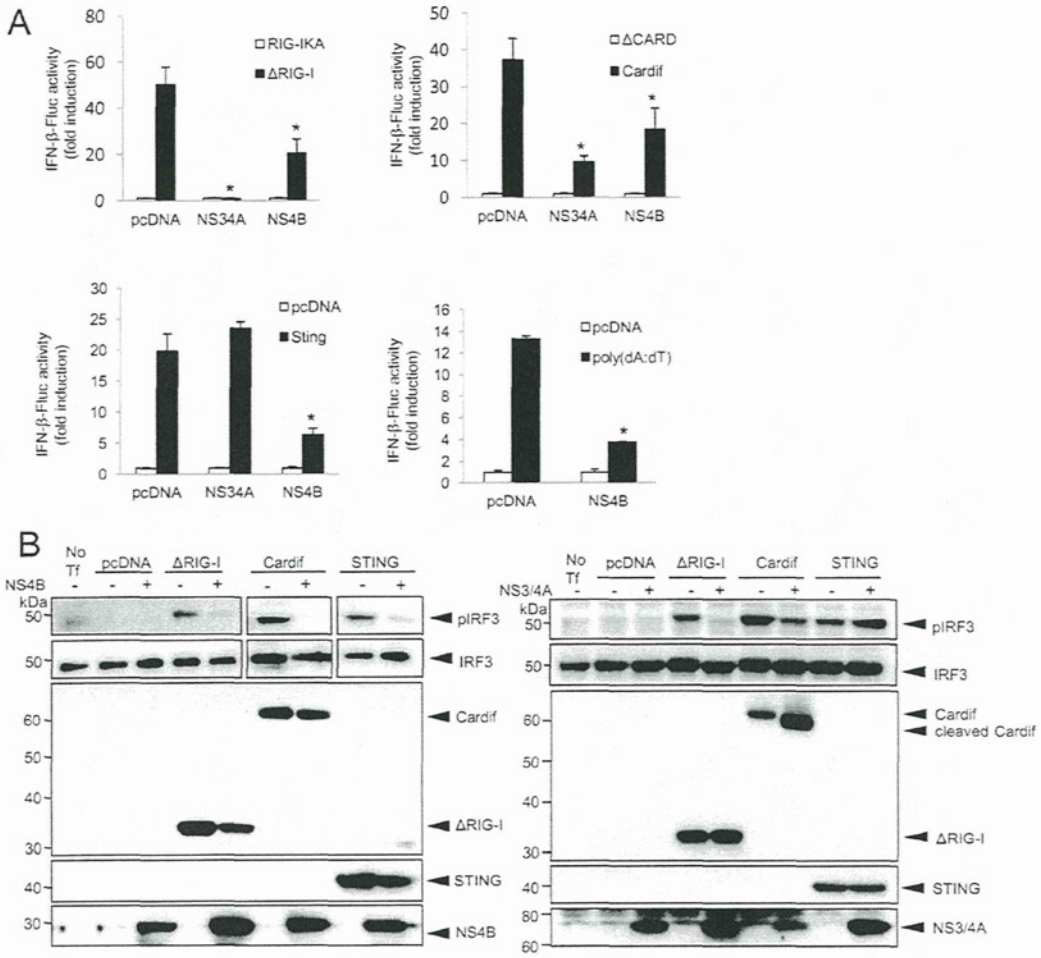

Fig. 1. NS4B suppressed IFN-β signaling mediated by RIG-I, Cardif, or STING. (A) Plasmids expressing ΔRIG-I, Cardif, or STING or poly(dA:dT) as well as NS3/4A or NS4B were cotransfected with pIFN-β-Fluc and pRL-CMV into HEK293T cells. After 24 hours, dual luciferase assays were performed. Plasmids expressing RIG-IKA, ΔCARD, or an empty plasmid (pcDNA) were used as a corresponding negative control. The experiments were performed more than three times and yielded consistent results. The *y* axis indicates relative IFN-β-Fluc activity. Assays were performed in triplicate and error bars indicate mean ± SD. $^*P < 0.05$. (B) HEK293T cells were cotransfected with indicated plasmids. On the day after transfection, the cells were lysed and immunoblot analyses were performed. No Tf, transfection-negative controls. pIRF-3 and IRF-3, phosphorylated and total IRF-3, respectively.

NS4B suppress RIG-I–mediated IFN-β production, but they do so by targeting different molecules in the signaling pathway.

Subcellular Localization of NS4B, Cardif, and STING. We next studied the subcellular localization of NS4B following its overexpression and measured the colocalization of NS4B with Cardif and STING in both HEK293T cells and Huh7 cells by indirect immunofluorescence microscopy. NS4B was localized predominantly in the ER, which is consistent with previous reports[33] (Fig. 2A). Cardif was localized in mitochondria but did not colocalize with the ER-resident host protein disulphide-isomerase (PDI). Interestingly, Cardif and NS4B colocalized partly at the boundary of the two proteins, although their original localization was different (Fig. 2A,C). STING was localized predominantly in the ER[20,21] (Fig. 2B,D). STING colocalized partly with Cardif, which is consistent with a previous report by Ishikawa and Barber[20] (Fig. 2B,D). In cells cotransfected with NS4B and STING expression plasmids, NS4B colocalized precisely with STING (Fig. 2B,D). To examine the region of NS4B-STING interaction, we next observed the two proteins by performing staining for them along with mitochondria-associated ER membrane (MAM), which is a physical association with mitochondria[34] and has been reported the site of Cardif-STING association.[24] Both NS4B and STING were adjacent to and partially colocalized

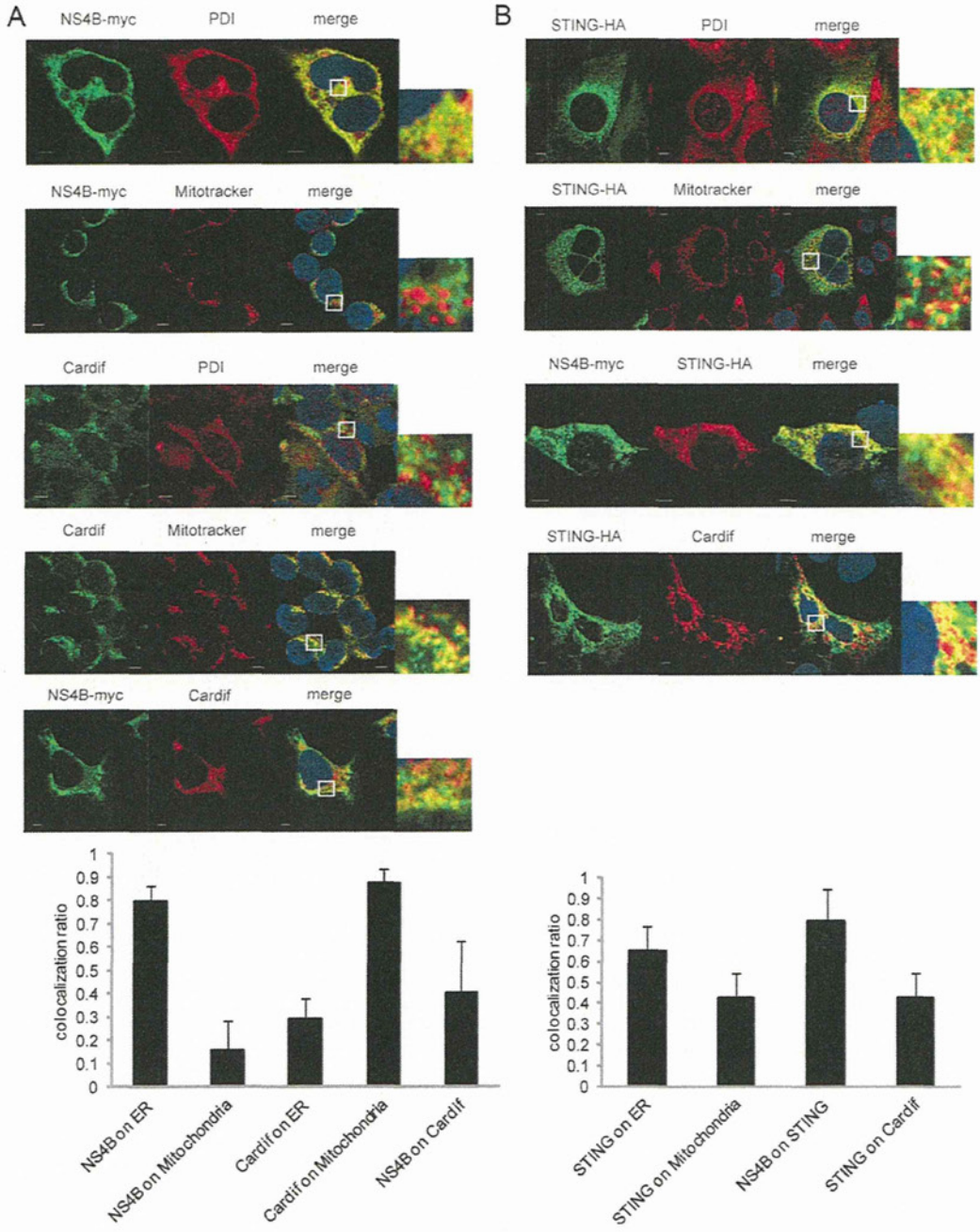

Fig. 2. Subcellular localization of NS4B, Cardif, and STING. (A-D) Subcellular localization of NS4B, Cardif, and STING in 293T (A,C) and Huh7 (B,D) cells. (A,C) NS4B-myc (first, second, and fifth panels of A and third panel of C) was transfected, and 24 hours later the cells were fixed and immunostained with anti-myc. In the third, fourth, and fifth panels of A, and the first and second panels of C, endogenous Cardif was detected with anti-Cardif antibody. ER was immunostained with anti-PDI antibody (first and third panels of A and first panel of C). Mitochondria were stained using Mitotracker (second and fourth panels of A and second panel of C). Nuclei were stained with 4',6-diamidino-2-phenylindole (DAPI). (B,D) STING-HA (all panels) and NS4B-myc (third panels) were transfected, and after 24 hours the cells were fixed and immunostained with anti-HA or anti-myc, respectively. In the fourth panels, endogenous Cardif was detected with anti-Cardif antibody. ER was immunostained with anti-PDI antibody (first panels). Mitochondria were stained using Mitotracker (second panels). Nuclei were stained with DAPI. (E) NS4B-myc and STING-HA were transfected into Huh7 cells and after 24 hours the cells were fixed and immunostained with anti-HA, anti-myc, and anti-FACL4 (MAM) antibody. Cells were visualized by confocal microscopy. Scale bars indicate 5 μm. In each microscopic image, the grade of protein colocalization in a single cell was quantified and is shown in the graphs at the bottom of each panel. Values are shown as the average colocalization ratio in 8 cells. Error bars indicate the mean + SD.

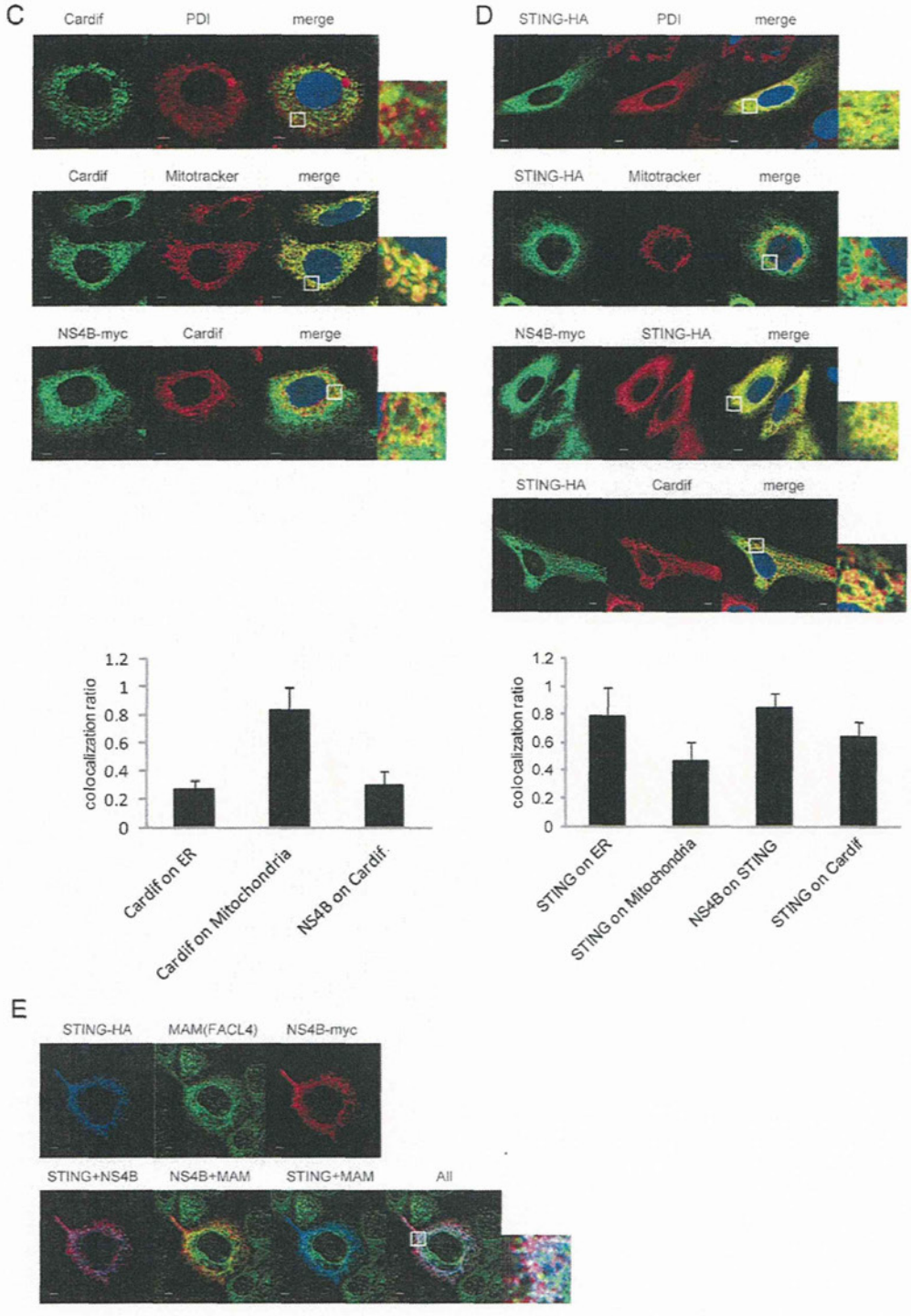

Fig. 2. Continued

with fatty acid-CoA ligase long chain 4 (FACL4), which is a MAM marker protein[35,36] (Fig. 2E). These findings suggest that NS4B might interact with STING on MAM more strongly than with Cardif.

Protein-Protein Interaction Between NS4B, Cardif, and STING. Knowing that NS4B was colocalized strongly with STING and only partly with Cardif, we next analyzed direct protein-protein interactions

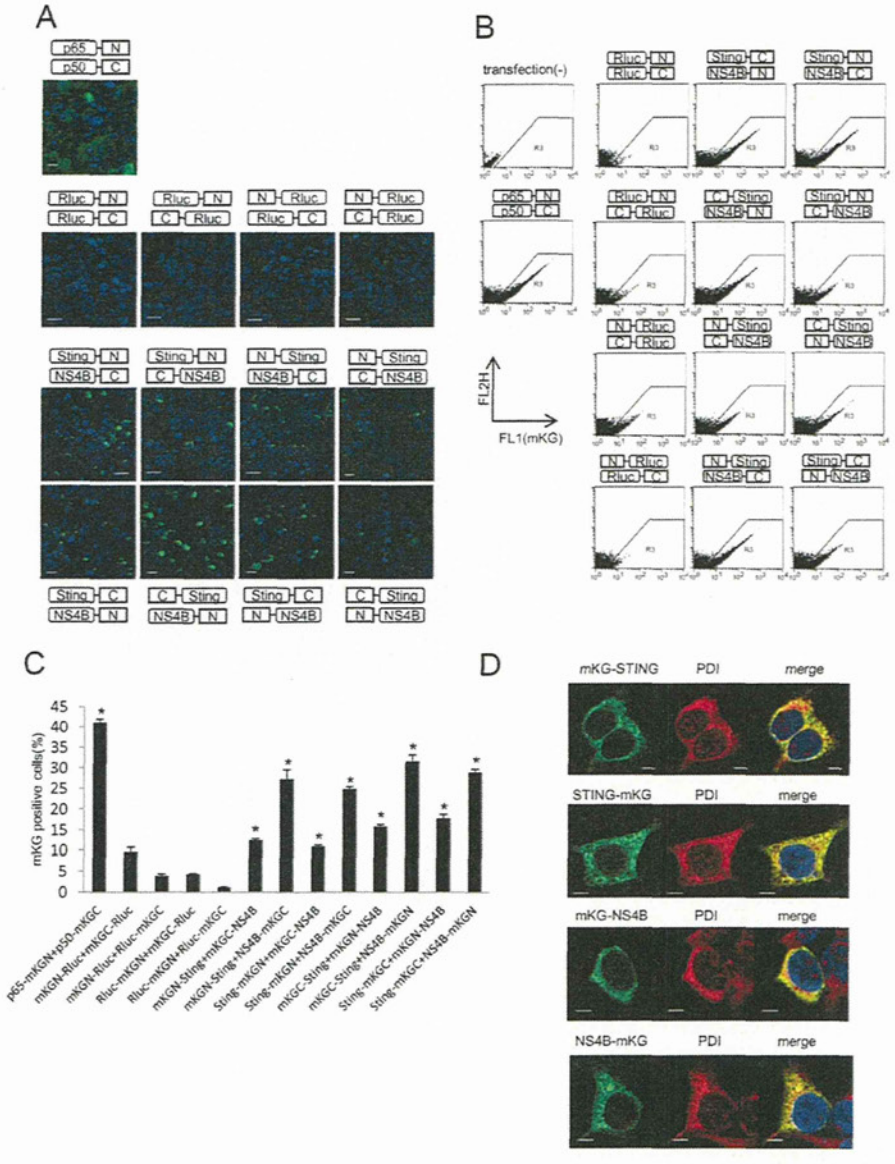

Fig. 3. BiFC assays of STING and NS4B. The complementary pairs of N- or C-terminally mKG-fused NS4B and STING expression plasmids were cotransfected in HEK293T cells. After 24 hours, the cells were fixed and observed by confocal microscopy (A) or subjected to flow cytometry to measure mKG-emitted fluorescence (BiFC signal) and to count BiFC signal-positive cells (B,C). Plasmids expressing p65-mKGN and p50-mKGC individually were used as a BiFC-positive control and plasmids expressing N- or C-terminally mKG fused Rluc were used as a negative control. The letters N and C denote complimentary N- and C-terminal fragments of mKG, respectively. Assays were performed in triplicate and error bars indicate the mean ± SD. Scale bars indicate 10 μm (A). *$P < 0.05$ compared with corresponding negative controls. (D) Plasmids expressing mKG fragment-fused STING or NS4B were transfected in HEK293T cells. After 24 hours, the cells were fixed and immunostained with anti-mKG and anti-PDI (ER) antibody. Nuclei were stained with DAPI. Cells were observed by confocal microscopy. Scale bars = 5 μm.

between NS4B, Cardif, and STING. To detect those interactions in living cells, we performed BiFC assays.[37,38] We constructed NS4B, Cardif, and STING expression plasmids that were N- or C-terminally fused with truncated mKG proteins, respectively. First, we cotransfected several different pairs of NS4B and STING expression plasmids that were fused with complementary pairs of N- or C-terminally truncated mKG. Strong fluorescence by mKG complexes (BiFC signal) was detected in all pairs of cotransfections, suggesting significant molecular interaction (Fig. 3A). In flow cytometry, all pairs of NS4B- and STING-mKG fusion proteins were positive for strong BiFC signal (Fig. 3B). The percentages of cells positive for BiFC signal were significantly higher in STING-mKG and NS4B-mKG fusion complexes than in corresponding controls (Fig. 3C). These results demonstrate that HCV-NS4B and STING proteins interact with each other strongly and specifically in cells. Fluorescence microscopy indicated that N- and C-terminal fusion of mKG onto NS4B and STING did not affect subcellular localization (Fig. 3D).

We next studied the molecular interaction between NS4B and Cardif by BiFC assay using NS4B and Cardif fusion plasmids that were tagged with complementary pairs of truncated mKG. Weak fluorescence was detected in cells transfected with the pairs N-Cardif and NS4B-C, N-Cardif and C-NS4B, C-Cardif and

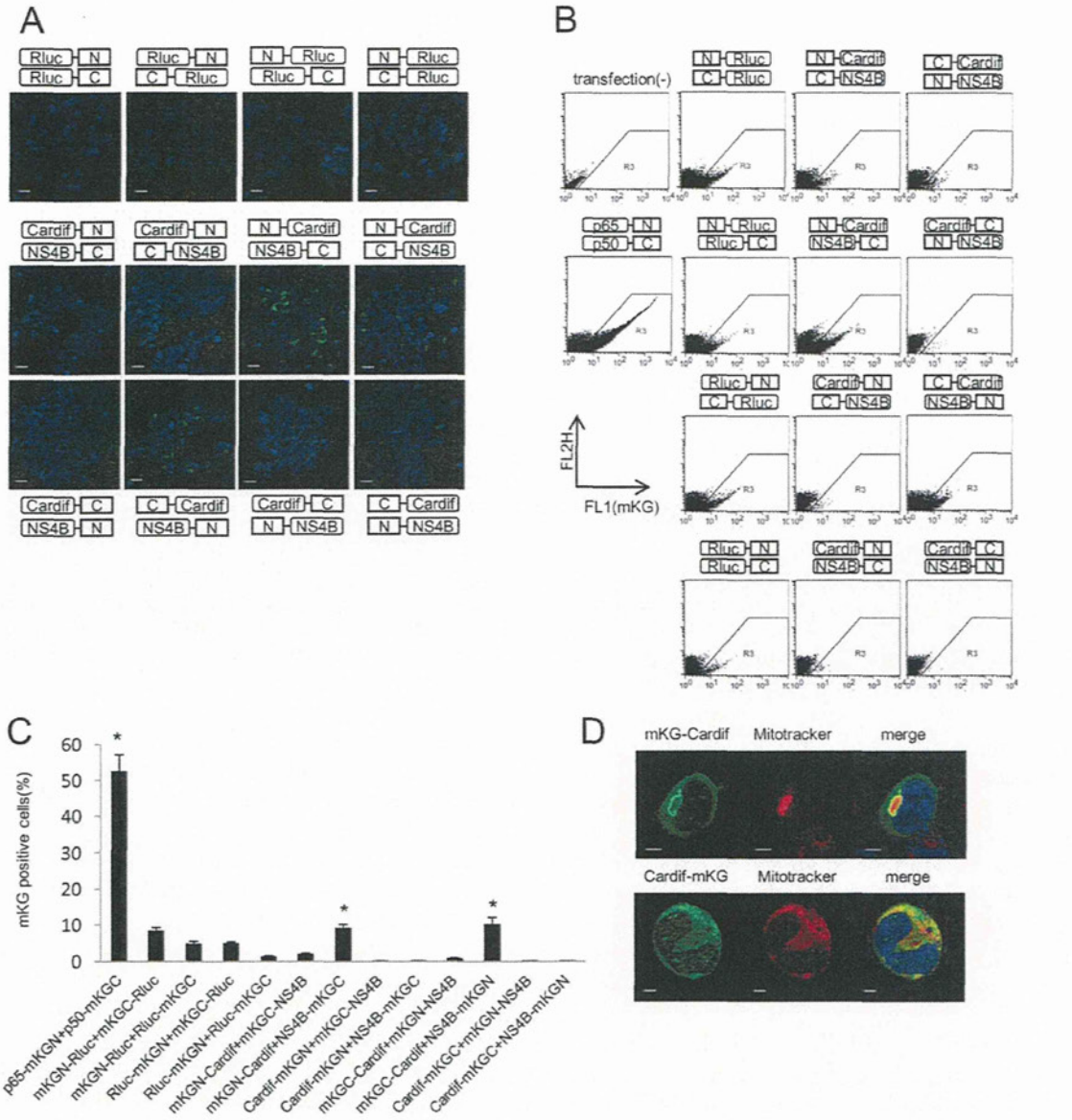

Fig. 4. BiFC assays of Cardif and NS4B. The complementary pairs of N- or C-terminally mKG-fused NS4B and Cardif expression plasmids were cotransfected in HEK293T cells. After 24 hours, the cells were fixed and observed by confocal microscopy (A) or subjected to flow cytometry to measure mKG-emitted fluorescence (BiFC signal) and to count BiFC signal-positive cells (B,C). Plasmids expressing p65-mKGN and p50-mKGC individually were used as a BiFC-positive control and plasmids expressing N- or C-terminally mKG-fused Rluc were used as a negative control. The letters N and C denote complimentary N- and C-terminal fragments of mKG, respectively. Assays were performed in triplicate, and error bars indicate the mean ± SD. Scale bars indicate 10 μm (A). *$P < 0.05$ compared with corresponding negative controls. (D) Plasmids expressing mKG fragment-fused STING or NS4B were transfected in HEK293T cells. After 24 hours, the cells were fixed and immunostained with anti-mKG antibody. Mitochondria were stained using Mitotracker, and nuclei were stained with DAPI. Cells were observed by confocal microscopy. Scale bars = 5 μm.

NS4B-N, and C-Cardif and N-NS4B (Fig. 4A,B). The percentage of cells positive for BiFC signal increased with the combination of N-Cardif and NS4B-C, and C-Cardif and NS4B-N (Fig. 4C). Fluorescence microscopy indicated that mKG-Cardif, but not Cardif-mKG, was partially colocalized with mitochondria, possibly due to disruption of mitochondria anchor domain by C-terminal fusion with mKG (Fig. 4D). These results indicate the lack of significant molecular interactions between NS4B and Cardif.

Binding of NS4B to STING Blocks Molecular Interaction Between Cardif and STING. It has been reported that STING binds Cardif directly.[20,22] Thus, we hypothesized that NS4B, through a competitive

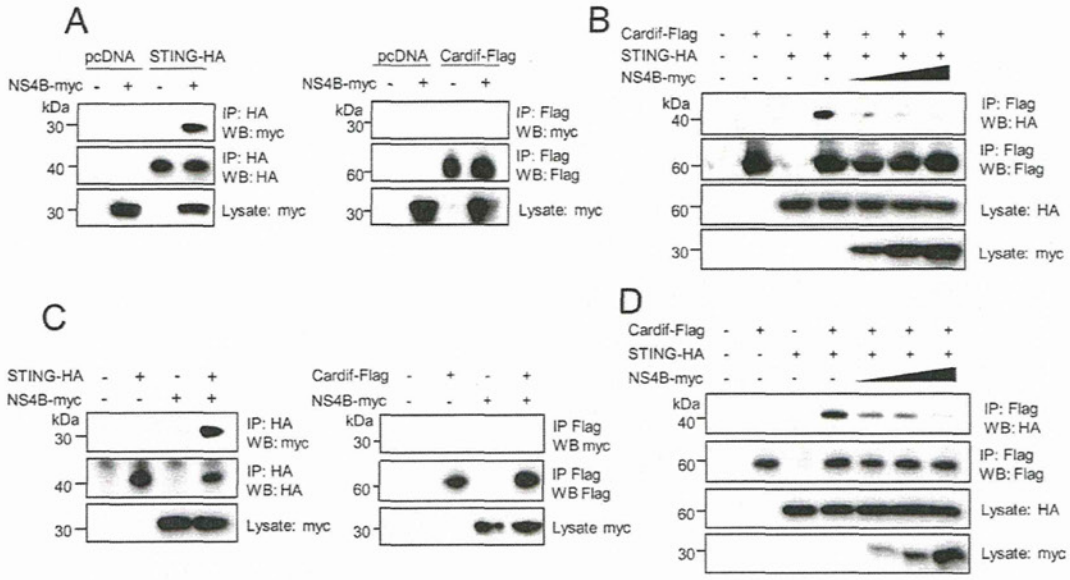

Fig. 5. Binding of NS4B to STING blocks molecular the interaction between Cardif and STING. (A,C) NS4B expression plasmid was cotransfected with STING or Cardif expression plasmid into HEK293T cells (A) or Huh7 cells (C). After 24 hours, cell lysates were subjected to immunoprecipitation using anti-HA or anti-Flag and were immunoblotted with anti-myc. (B,D) Cardif and STING expression plasmids were cotransfected with various amounts of NS4B plasmid in HEK293T cells (B) or Huh7 cells (D). After 24 hours, cells lysates were subjected to immunoprecipitation using anti-Flag and were immunoblotted with anti-HA.

interaction with STING, may hinder the direct molecular interaction between Cardif and STING. To verify this hypothesis, we performed immunoprecipitation assays. First, we transfected plasmids that expressed NS4B and Cardif, or NS4B and STING, in HEK293T cells or Huh7 cells, and performed immunoprecipitation. NS4B strongly bound to STING in both HEK293T cells and Huh7 cells, suggesting specific molecular interactions, whereas NS4B and Cardif did not show any obvious interaction (Fig. 5A,C). Consistent with previous reports, STING and Cardif showed significant interaction (Fig. 5B,D). Interestingly, those interactions were decreased by coexpression of NS4B, depending on its input amount, and finally blocked completely in both HEK293T and Huh7 cells (Fig. 5B,D). Collectively, the results above demonstrate that NS4B disrupts the interaction between Cardif and STING possibly through competitive binding to STING.

Effects on HCV Infection and Replication Levels by STING Knockdown and NS4B Overexpression. We next studied the impact of STING-mediated IFN production and its regulation by NS4B on HCV infection and cellular replication. First, we transfected three STING-targeted siRNAs into Huh7/Feo cells (Fig. 6A). As shown in Fig. 6B, STING knockdown cells conferred significantly higher permissibility to HCV replication. We next transfected HCV-JFH1 RNA into Huh7 cells that were transiently transfected with NS4B. As shown in Fig. 6C, HCV core protein expression was significantly higher in NS4B-overexpressed cells. Furthermore, HCV replication was increased significantly in Huh7/Feo cells overexpressing NS4B (Fig. 6D). Taken together, the results above demonstrate that STING and NS4B may negatively or positively regulate cellular permissiveness to HCV replication.

The N-terminal Domain of NS4B Is Essential for Suppressing IFN-β Promoter Activity Mediated by RIG-I, Cardif, and STING. It has been reported that the N-terminal domain of several forms of flaviviral NS4B shows structural homology with STING.[24] We therefore investigated whether the STING homology domain in NS4B is responsible for suppression of IFN-β production. We constructed two truncated NS4B expression plasmids, which covered the N terminus (NS4Bt1-84, amino acids 1 through 84) containing the STING homology domain and the C terminus (NS4Bt85-261, amino acids 85 through 261), respectively (Fig. 7A). Immunoblotting showed that NS4Bt1-84 and NS4Bt85-261 yielded protein bands of ~9 kDa and ~20 kDa, respectively. Aberrant bands in the truncated NS4B may be due to alternative posttranslational processing. HEK293T cells were transfected with ΔRIG-I, Cardif, or STING, and NS3/4A or the truncated NS4B, along with IFN-β-Fluc plasmid, and a reporter assay was performed. NS4Bt1-84 significantly suppressed RIG-I, Cardif, and STING-

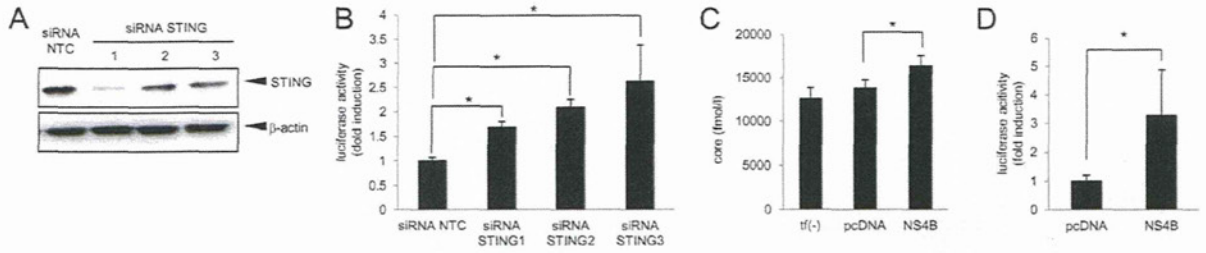

Fig. 6. Effects on HCV replication levels by STING knockdown and NS4B overexpression. (A) Effects of siRNA knockdown of STING by siRNA. Huh7 cells were transfected with STING-targeted siRNAs (siRNA STING-1, -2, and -3, respectively) or negative control siRNA (siRNA NTC). Seventy-two hours after transfection, cells were harvested and expression levels of STING protein were detected by immunoblotting. (B) Huh7 cells expressing HCV-Feo subgenomic replicon (Huh7/Feo)[27,28] were transfected with STING-targeted siRNAs or negative control siRNA. Seventy-two hours after transfection, cells were harvested, and internal luciferase activities were measured. The *y* axis indicates luciferase activity shown as a ratio of transfection-negative control. Assays were performed in triplicate, and error bars indicate the mean + SD. $*P < 0.05$ compared with corresponding negative controls. (C) Empty plasmid or plasmid expressing NS4B was transfected into Huh7 cells. After 24 hours, HCV-JFH1 RNA was transfected into these cells. Seventy-two hours after virus transfection, HCV core antigen levels in culture medium were measured. Assays were performed in triplicate, and error bars indicate the mean + SD. $*P < 0.05$ compared with corresponding negative controls. tf(−), transfection-negative control. (D) Huh7 cells expressing HCV-Feo replicon (Huh7/Feo)[27,28] were transfected with NS4B expressing plasmid or empty plasmid (pcDNA). Forty-eight hours after transfection, internal luciferase activities were measured. The *y* axis indicates luciferase activity shown as a ratio of the transfection-negative control. Assays were performed in triplicate, and error bars indicate the mean + SD. $*P < 0.05$ compared with corresponding negative controls.

induced IFN-β promoter activity, whereas NS4Bt85-261 did not (Fig. 7B). These results suggest that the N-terminal domain of NS4B is responsible for association with STING. Fluorescent microscopy indicated that both NS4Bt1-84 and NS4Bt85-26 colocalized with ER and STING (Fig. 7C).

NS4B Suppresses IFN Production Signaling Cooperatively with NS3/4A. It has been reported that

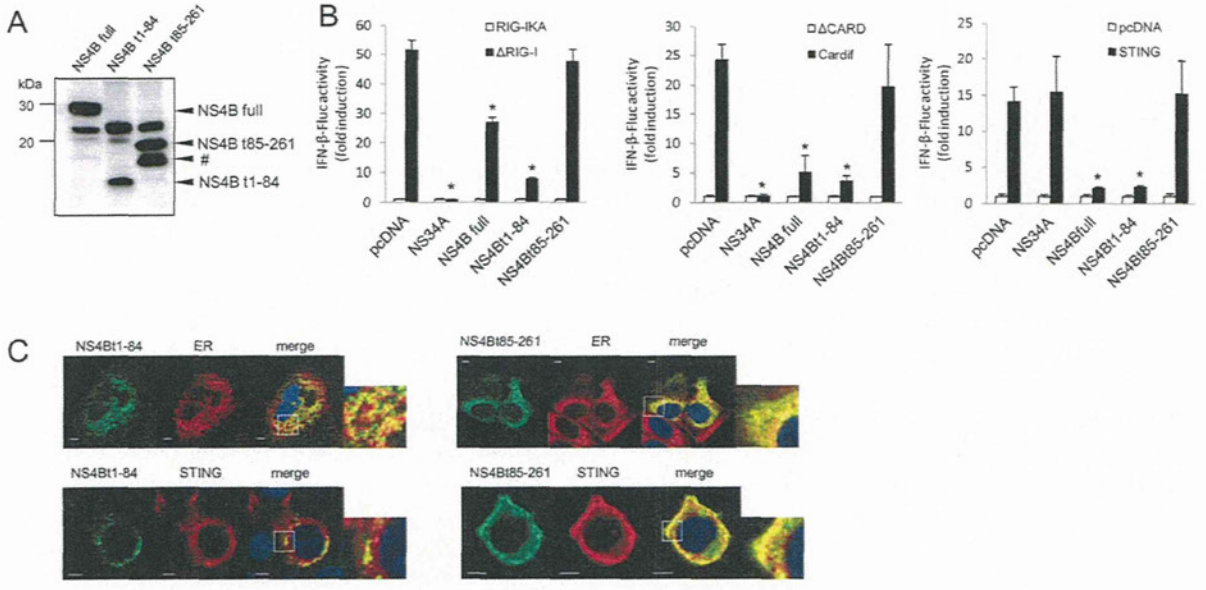

Fig. 7. The N-terminal domain of NS4B is essential for suppressing IFN-β promoter activity induced by RIG-I, Cardif, or STING. (A) Immunoblotting of NS4B and truncated NS4B, NS4B t1-84, and NS4Bt85-216. HEK293T cells were transfected with NS4B or truncated NS4B. After 24 hours, the cells were lysed and immunoblot assays were performed. The band indicated by the pound sign (#) is a truncated NS4B, probably generated via alternative posttranslational processing. (B) Plasmids expressing ΔRIG-I, Cardif, or STING as well as NS3/4A or the indicated truncated form of NS4B were cotransfected with pIFN-β-Fluc and pRL-CMV in HEK293T cells. Dual luciferase assays were performed 24 hours after transfection. Plasmids expressing RIG-IKA, ΔCARD, or pcDNA were used as negative controls. The *y* axis indicates IFN-β-Fluc activity shown as relative values. Assays were performed in triplicate, and error bars indicate the mean ± SD. $*P < 0.05$ compared with corresponding negative controls. (C) Plasmids expressing NS4Bt1-84-myc of NS4Bt85-261-myc were transfected with or without plasmids expressing HA-STING in HEK293T cells. After 24 hours, the cells were fixed and immunostained. Nuclei were stained with DAPI. Cells were observed by confocal microscopy. Scale bars indicate 5 μm.

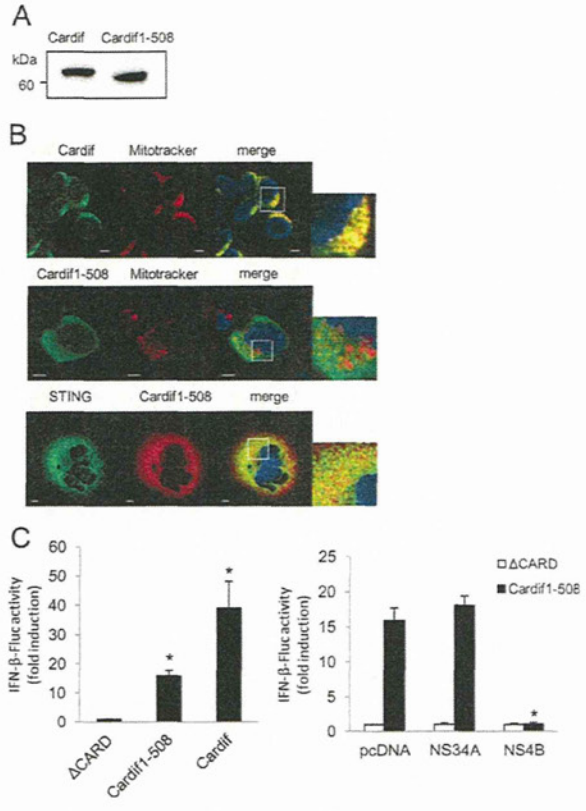

Fig. 8. NS4B suppressed IFN-β production pathway independently of and cooperatively with NS3/4A. (A) Immunoblotting of Cardif and truncated Cardif (Cardif1-508). HEK293T cells were transfected with Cardif or truncated Cardif (Cardif1-508). After 24 hours, the cells were lysed and immunoblot assays were performed. (B) Subcellular localization of Cardif and truncated Cardif (Cardif1-508). HEK293T cells were immunostained with anti-Cardif antibody or HEK293T cells were transfected with myc-tagged truncated Cardif (Cardif1-508-myc), and after 24 hours the cells were immunostained with anti-myc. Mitochondria were stained with Mitotracker (red) and nuclei were stained with DAPI (blue). Plasmid expressing myc-tagged truncated Cardif (Cardif1-508) and plasmid expressing HA-tagged STING were transfected into HEK293T cells. The cells were immunostained with anti-myc and anti-HA antibodies and analyzed by confocal laser microscopy. Scale bars = 10 μm. (C) Plasmids expressing Cardif or truncated Cardif (Cardif1-508) and pIFN-β-Fluc and pRL-CMV were transfected with or without plasmid expressing NS3/4A or NS4B into HEK293T cells as indicated. Dual luciferase assays were performed 24 hours after transfection. Plasmid expressing ΔCARD or pcDNA was used as a negative control. The *y* axis indicates IFN-β-Fluc activity shown as relative values. Assays were performed in triplicate, and error bars indicate the mean ± SD. $^*P < 0.05$.

HCV NS3/4A serine protease cleaves Cardif between Cys-508 and His-509, releases Cardif from the mitochondrial membrane, and blocks RIG-I–induced IFN-β production. We next assessed whether NS4B suppresses IFN-β production in the presence of Cardif cleaved by NS3/4A protease (Cardif1-508, Fig. 8A). The truncation of Cardif–C-terminal residue abolished mitochondrial localization but still colocalized with STING (Fig. 8B). The reporter assay showed that Cardif1-508 induced weak IFN-β activation. Interestingly, NS4B completely blocked the residual function of the Cardif1-508 protein to activate IFN-β expression, suggesting an additive effect of NS3/4A and NS4B on the RIG-I–activating pathway (Fig. 8C).

Discussion

It has been reported that viruses, including HCV, target IFN signaling to establish persistent replication in host cells.[39] We have reported that NS4B blocks the transcriptional activation of ISRE induced by overexpression of RIG-I and Cardif, but not by TBK1 or IKKϵ.[19] In the present study, we have shown that NS4B directly and specifically binds STING, an ER-residing scaffolding protein of Cardif and TBK1 and an inducer of IFN-β production (Figs. 3 and 5), and blocked the interaction between STING and Cardif (Fig. 5B,D) resulting in strong suppression of RIG-I–mediated phosphorylation of IRF-3 and expressional induction of IFN-β (Fig. 1). Furthermore, HCV replication was increased by knockdown of STING or overexpression of NS4B (Fig. 6). Taken together, our results demonstrate that HCV-NS4B strongly blocks virus-induced, RIG-I–mediated activation of IFN-β production signaling through targeting STING, which constitutes a novel mechanism of viral evasion from innate immune responses and establishment of persistent viral replication.

Our results also showed that the effects of NS4B on the RIG-I signaling were independent of NS3/4A-mediated cleavage of Cardif. Reporter assays showed that a cleaved form of Cardif (Cardif1-508) partially retained activity for the induction of IFN-β promoter activation. The residual IFN-β promoter activation was suppressed almost completely by NS4B but not by NS3/4A (Fig. 8C). These findings show that there are at least two mechanisms by which HCV can abrogate RIG-I–mediated IFN production signaling to accomplish abrogation of cellular antiviral responses.

NS4B and STING are ER proteins,[20,21,40] whereas Cardif is localized on the outer mitochondrial membrane.[9] Consistent with those reports, our immunostaining experiments demonstrated that most NS4B protein colocalized with STING (Fig. 2), and their association was localized on MAM (Fig. 2E). In addition to the significant colocalization of STING and NS4B, STING partially colocalized with Cardif at the boundary region of the two proteins (Fig. 2B). Furthermore, immunoprecipitation experiments showed that overexpression of NS4B completely blocked the interaction of STING with Cardif (Fig. 5B). Ishikawa et al.[24] reported